University of Nevada, Reno

Design and Implementation of Pattern Recognition Algorithms for the Detection of Chemicals with a Microcantilever Sensor Array

A thesis submitted in partial fulfillment of the
requirements for the degree of Master of Science in
Computer Science

by

Asya F. Nikitina

Dr. Monica Nicolescu/Thesis Advisor

December, 2007

University of Nevada, Reno
Statewide • Worldwide

THE GRADUATE SCHOOL

We recommend that the thesis
prepared under our supervision by

ASYA F. NIKITINA

entitled

Design and Implementation of Pattern Recognition Algorithms for the Detection of Chemicals with a Microcantilever Sensor Array

be accepted in partial fulfillment of the
requirements for the degree of

MASTER OF SCIENCE

Monica Nicolescu, Ph.D., Advisor

Mircea Nicolescu, Ph.D., Committee Member

Joseph I. Cline, Ph.D., Graduate School Representative

Marsha H. Read, Ph. D., Associate Dean, Graduate School

December, 2007

Abstract

Nowadays, we are witnesses to the noticeable success in the development of a new class of chemical and biological sensors – microfabricated cantilever sensor arrays actuated at their resonance frequencies and functionalized by polymer coatings. The major advantages of such miniature sensors are their small size, fast response, remarkably high sensitivity, and the endless possibilities of reaching high selectivity via customized combination of polymer coatings. These devices are inexpensive, portable, and have the ability to operate in various environments, such as vacuum, air and liquids. The areas of applications of microfabricated cantilever sensor arrays are almost countless, including a variety of scientific research in physics, chemistry, biochemistry, biology, and genetics, food and beverage industry, perfume industry, pharmacology, medicine, environmental monitoring, and most recently, related to the national security due to a high risk of terrorist attacks.

However, despite the remarkable achievements in fabrication of microcantilever sensor arrays, creating an accurate and reliable pattern recognition algorithm as a part of the sensory system is still an essential and not yet completely solved problem. Most pattern analysis algorithms that have been used with the cantilever sensor arrays today are highly customized, *ad hoc* algorithms. They often lack generality and cannot be easily carried from one set of experimental data to another. Therefore, the main goal of the current work was developing a pattern recognition algorithm that can be highly effective on a given set of sensory data and easily adjustable to any new set of data.

Acknowledgments

I would like to take this opportunity to express my most sincere gratitude to my research advisor at the University of Nevada, Reno, Dr. Monica Nicolescu for giving me the opportunity to work in her research group, for her guidance, constant support, and help.

I greatly thank Dr. Joseph Cline for helping me with my research project and Dr. Mircea Nicolescu for helping me with my thesis. I also thank both Dr. Joseph Cline and Dr. Mircea Nicolescu for spending their valuable time to read my thesis.

Thanks to Dr. Carl Looney for exposing me to fuzzy systems and neural networks. I also thank Dr. Jesse Adams and Ben Rogers from Nevada Nanotech System, Inc. for giving me the opportunity to work in their lab and for their help with the experimental part of the project.

Thanks to our research group members: Chris King, Sebastian Smith, and Austin Stanhope for their help. Also thanks to Jihyo Chong for helping me to collect the experimental data.

Financial support by an NSF-EPSCoR Sensors fellowship is greatly acknowledged.

1 Introduction

There always has been a high interest in developing micromechanical devices for analyte detection for various applications such as quality and process control in industry, disposal diagnostics for biomedical analyses, pharmacological screening, gas sensing devices for environmental and health-related agencies, forensic investigations, fragrance design, and many others. Recently, the new threat of international terrorism brought the urgency for developing such sensor devices to a new high level. The new demand brought new requirements: now not only should sensors be highly sensitive to a wide range of target analytes, but they should also be miniaturized, automated, cost effective, reliable and robust.

The concept of chemical and biochemical sensors has been a subject of extensive research efforts for a long time. The conventional approach to chemical sensors traditionally uses an approach called “lock-and-key” design, where a specific receptor is synthesized for each analyte of interest. This type of sensors is extremely selective, but usually quite expensive and has limited potential to meet today’s real-life demand for detection of a broad range of analytes with the same sensor device.

A new revolutionary approach to chemical and biochemical sensors is closer conceptually to our own sense of olfaction. In this approach, instead of the strict “lock-and-key” single sensor design architecture, an array of different sensors, each of which responds to different chemicals or even different classes of chemicals is used [1], [2], [3]. The idea behind this design is that the sensors of this array should contain as much

detection diversity as possible, so the array itself responds to the largest range of analytes. It is important to stress that in this design often none of the sensors that comprise the array is able to identify any analyte on its own, as a single element; only a specific pattern of responses from all sensors in the array provides the information that allows classification and identification of that particular analyte.

Today, the emerging new technology based on microfabricated cantilever sensor arrays represents an ideal sensor technology that offers potential solutions to exponentially growing real-life problems regarding the fast and reliable detection of small concentration of target analytes in the air and solutions. Such miniaturized cantilever sensor arrays have already proven to be highly useful and appropriate as chemical and biological sensors for detecting traces of target analytes in both gaseous and liquid media [4], [5], [6], [7].

In order to be used as chemical and biochemical sensors, one side of the cantilevers is often coated with some functional layer that might be either *highly* specific or *partially* specific. The layer is considered to be highly specific if it is designed to recognize some particular target analyte normally by irreversibly reacting with it; the layer is considered to be partially specific if it adsorbs (and later releases) a broad range of target analytes at different rates. In the latter case, it is possible to recognize individual analytes from a list of numerous target analytes with the same cantilever sensor array. Thus, arrays offer greater selectivity than single sensors, since the response patterns of an array of semiselective sensors contain much more information than the responses of any single sensor. Needless to say, the selection of the coating materials for different

cantilevers in the array, in order to increase the sensor array's ability to detect a larger number of individual analytes or to analyze mixtures, is yet another challenge that this sensor technology faces today [8].

The response of the cantilever array has to be analyzed via some pattern recognition technique, which aims to facilitate the application of the device as a reliable and inexpensive sensing system. Today, pattern recognition is a critical part of the development of the micromechanical cantilever arrays of sensors capable of detecting, identifying and sometimes quantifying the target chemical and biological substances. The successful design process involves a careful consideration of a lot of different issues, such as signal preprocessing, feature extraction, feature filtering and selection, designing of the pattern analysis system, training the system, and finally performing recognition of future (unseen before) samples and assessing the results of system's classification accuracy [9].

There were several objectives of the current work.

The first objective was to design and conduct a series of experiments with a microfabricated cantilever sensor array by exposing it to a set of target analytes. During this stage of the research, we explored the effects of different coating materials, heating and cooling the array cell, and the different concentrations of the analytes in the air on the collected sensory data.

The second objective of our work was to develop the process of feature extraction and selection. In order to create a successfully functioning detection system, we had to

carefully choose the adequate number of features and ensure that those features are both unique and sufficient to characterize each collected sample during the experiment.

The final and most important objective of the current work was to develop a number of suitable pattern recognition algorithms for our specific sensory data, test those algorithms using the benchmark data sets and data collected within framework of the current research, compare their efficiency and accuracy, and make necessary assessment of their power and suitability for the detection of the target analytes with a microcantilever sensor array in the real-life situations.

This thesis is structured as follows:

- **Chapter 2 – Related Work**: presents a review of the current progress in the field of the microcantilever sensor array technology. It also describes the types of pattern recognition algorithms that are often used in combination with microcantilever sensor arrays for the detection and qualitative and quantitative identification of a wide range of the target analytes.
- **Chapter 3 – Experimental Setup**: describes the details of the experiments conducted with a microcantilever sensor array, shows some pictures of the array's responses, and explains the strategy of the feature extraction procedure.
- **Chapter 4 – Theory and Algorithms Details**: presents a theoretical background and detailed description of all pattern recognition algorithms that were designed and implemented in the current research. It also shows the testing results of classification accuracy for each algorithm using a benchmark data set (the Wisconsin breast cancer data set).

- **Chapter 5 – Experimental Results**: contains the results of each algorithm's performance on the experimental sensory data collected in the Nevada Nanotech System, Inc. (NNTS) laboratory using a microfabricated cantilever sensor array.
- **Chapter 6 – Conclusion and Future Work**: summarizes the performance results of all pattern recognition algorithms on the given sensory data set and provides some suggestions for future work in the most promising directions.

2 Related Work

Microcantilevers constitute a special class of sensors – *mechanical* sensors, also called *deflection* sensors, meaning that those sensors respond to changes of external parameters, such as temperature changes or molecule adsorption, by a mechanical response, e.g., by bending or deflection.

The term *cantilever* means a microfabricated rectangular bar-shaped structure, whose length is much greater than its width, and thickness is much smaller than both its lengths and width. Cantilever beams have been used to measure interatomic forces in the piconewton range using a technique called scanning force microscopy (SFM) or atomic force microscopy (AFM) since the mid 1980's [10]. It turned out that microcantilevers were exceptionally sensitive to extremely low external forces or remarkably small mass displacements, that is, they were found to be very sensitive to external physical and chemical influence. Microcantilevers can operate in several modes, the most often used modes are static and dynamic modes, and potentially provide mass detection at the single molecule level.

In static mode [11], [12], [13], the cantilever surface (or a coating material of the upper surface of a cantilever) adsorbs molecules from the environment and the surface stress occurring during the adsorption results in a static bending of the cantilever and can be measured.

In dynamic mode [11], [14], [15], [16], each cantilever in the array is driven into oscillation externally at its unique resonance frequency. The cantilevers may be coated as

well. On the adsorption of the molecules from the surrounding medium, the resonance frequencies of each cantilever decrease due to the adsorbed mass. Those resonance frequency shifts can be measured and the adsorbed mass on the cantilever can be calculated.

The key to the high sensitivity of the microcantilevers is the very large surface-to-volume ratio, which leads to amplified surface stress.

The ability to use the arrays of sensors functionalized differently adds to the list of their advantages even more, by providing high selectivity toward certain classes of chemical and biological analytes. Arrays provide more useful and reliable information, since using many cantilevers in the same experiment opens up the possibility of exposing several differently functionalized cantilevers and reference cantilevers under identical conditions, i.e., several experiments can be performed at the same time. Additionally, none of the sensors in the array has specific selectivity to a given analyte, while it is often the case that the collective response from all sensors in the array provides the unique pattern that allows classification and identification of that particular analyte.

As was said before, in dynamic mode, the cantilever oscillates at a resonance frequency (the cantilever is driven into oscillation by some external circuitry). Analyte molecules adsorb to the active layer on the cantilever, increasing the mass of the vibrating cantilever and therefore, causing a light shift in the cantilever vibration frequency, very well measurable by external means. By measuring the resonance frequency sifts, the cantilever array can register a wide range of analyte concentrations in the surroundings.

In order to recognize a variety of analytes, or the different individual components in the mixture of analytes, each cantilever in the array should be coated with a different material that shows specific response (selectivity) to a particular class of analytes. Therefore, when arrays are used, it is preferable to use several different coating materials, each with somewhat different selectivity toward different classes of analytes. This approach maximizes the collection of the relevant sensor information for detecting and recognizing the analytes of interest. Due to this, there is high need of polymers suitable as coating materials for microcantilever sensors, with good physical and chemical properties for rapid and reversible analyte adsorption.

Both physical and chemical properties of coating polymers are equally important in making a good sensor. While the chemical properties determine the selectivity of the sensor to a particular analyte (or a class of analytes), the physical properties play an important role in other aspects of the performance, such as response time or refreshment time [8].

A wide variety of polymers has been studied and employed as suitable coating materials for microcantilever sensors to modify their sensitivity and selectivity to the target analytes. Some of the commercially available polymers that have been used in the current work are the following [8], [17], [18]:

1) PDMS (polydimethylsiloxane) – nonpolar polymer:

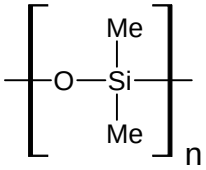

It is known to be useful for adsorbing aliphatic hydrocarbons or for distinguishing between members of a homologous series.

2) BSP3 (phenolic and trifluoromethyl groups added to dimethylsiloxy-polymer chain) – strong hydrogen bond acidic polymer:

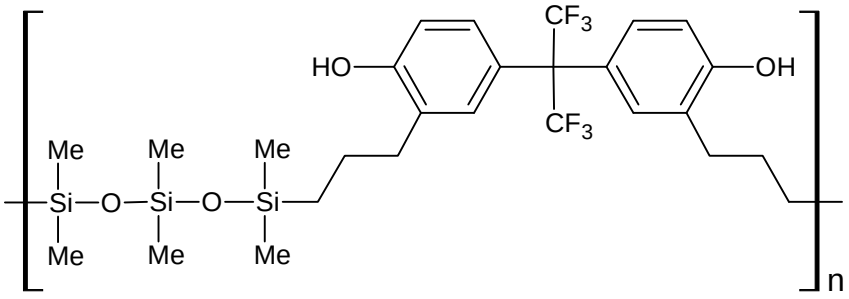

This type of material is useful in detection of basic vapors including organophosphorus compounds (some nerve agents are in that category).

3) OV-275 (poly(biscyanoallyl)siloxane) – dipolar moderately basic polymer:

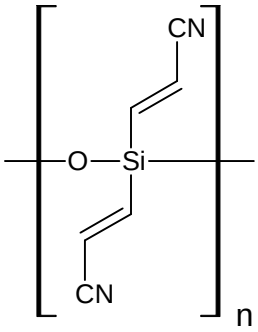

This polymer helps to distinguish vapors with a large dipole moment.

4) PECH (poly(epichlorohydrin)) – moderate dipolar polymer, contains moderate hydrogen-bonds:

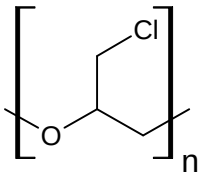

This coating material appears to be good at detecting aromatic hydrocarbons, such as benzene and toluene.

In addition to the demand of using different coating materials for different cantilevers within an array, normally at least one cantilever should be left uncoated to

serve as internal reference. All these factors and an extremely small size of the cantilevers themselves constitute a great challenge to functionalize cantilevers in the array individually [19]. There are not many suitable technologies available to do that. Among the most successful ones are coating the cantilevers using electrospray [20], [21] and inkjet printing [22]. The latter method was used in the process of functionalization of the cantilever sensor array used and tested in the current work (coating of the array cantilevers was performed by the Nevada Nanotech System, Inc. (NNTS) staff).

Several methods to monitor cantilever deflection have been successfully used in a measurement setup for cantilever arrays. These methods include optical (external laser) detection [23], [24], integrated piezoresistive detection [25], [26], integrated capacitive sensing [27], [28], and piezoelectric methods [29], [30], [31]. Piezoelectric cantilevers are ideal for resonance, frequency-based approaches – they do not require external optics or actuators, have low-power consumption, and allow actuating each cantilever in the array independently and directly. Therefore, the piezoelectric cantilever sensor array was used in the current work [32].

Creating sensitive, selective, reliable, robust, low-power and low-cost microcantilever sensor arrays is only a part of the solution to the global problem of detection of the target chemical and biological substances. Without dependable, fast, and accurate pattern recognition algorithms we would not be able to use such devices for the detection of any analytes of interest. Thus, the most important and crucial part in the development of a sensor array capable of detecting, identifying, and measuring the target analytes remains the development of a suitable pattern recognition algorithm.

The goal of a pattern recognition algorithm is to generate a class label prediction for a previously unseen sample from a set of class labels learned during the training phase of the algorithm. Obviously, in order to be able to recognize an analyte, the pattern recognition algorithm should be trained on a sufficiently large set of data. By data here we mean the output of any observation or measurement recorded by the cantilever sensor array under exposure to the target analyte (or a mixture of analytes) and by sufficient data we mean that in general, it is desirable that the algorithm be introduced to samples from all possible classes or categories. Then, by exploiting the knowledge extracted from the training data, the learning algorithm should be capable of adapting itself to infer a solution to the task of recognizing a new sample as belonging to some previously seen class (or several classes).

Perhaps the most widely exploited pattern recognition algorithms used in combination with cantilever sensor arrays are principal component analysis (PCA) [33], [34], [35], [36], [37] and a variety of neural networks (ANNs) [34], [36], [38], [39], [40]. In all cases satisfactory classification results were reported.

Principal component analysis extracts features from the observed data that exhibit the most dominant deviations in responses to various analytes. This procedure is aimed at maximum distinction performance between analytes. PCA in combination with cantilever sensor arrays was used, for example, to detect primary alcohols in gaseous mixtures [34], to detect and recognize vapors of dichloromethane, ethanol, toluene, and water in the air, and also perfume essences and beverage flavor [35], to detect different individual components such as methanol and 2-propanol in their binary mixtures [36]. PCA was also

used to find the best coating materials (out of 27) to successfully recognize one out of 14 analytes [37] – it has been found that only 7 different coating materials are required to discriminate among those 14 analytes.

For more complex measurements, e.g. to analyze multicomponent mixtures of gaseous analytes such as natural flavors, a different strategy involving artificial neural networks is pursued. Whereas PCA extracts most-dominant differences in the fingerprint pattern, neural network analysis considers all components of the fingerprints. Among the most interesting examples of the use of artificial neural networks are the detection and identification of different odorants (organic vapors such as amyl acetate, acetoin, menthone, and some aliphatic alcohols) [39], the identification of organic solvents in binary mixtures (*n*-octane – chloroform, *n*-octane – *n*-propanol, chloroform – *n*-propanol) [40]. The results for classification accuracy obtained by neural networks vary greatly, between 70% and 100%.

Among other pattern recognition techniques reported to be used in combination with cantilever sensor arrays is principal component regression (PCR) that was used, for example, for the quantitative prediction of organic vapors of octane, toluene, ethanol, and butylamine in the binary mixtures; the prediction error of 11.8%–12.5% is reported [41] and for quantitative and qualitative analysis of organic vapors of *n*-octane, 1-butanol, and toluene in binary mixtures high accuracy of the detection is reported [42].

The fuzzy *c*-means clustering algorithm (FCM) was used for the discrimination of organic compounds (14 different analytes total) [43]. The fuzzy *c*-means algorithm has

been found to perform better than PCA in discriminating analytes with similar structure, such as benzene and toluene, homologous alcohols, and acyclic aliphatic hydrocarbons.

Some modifications of PCA for multivariate data for the application to sensor arrays, such as Independent Component Analysis (ICA) – for the detection of different concentration of propanol and ethanol [44] and for identifying the concentration of carbon dioxide and hydrogen in the mixture [45], and Principal Discriminant Analysis (PDA) – for the discrimination among five varieties of roasted coffee beans are also reported [46]. The results of classification accuracy for ICA were reported as satisfactory, whereas PDA performed only with 64% of classification rate on coffee beans.

3 Experimental Setup

3.1 Experimental Setup

The experimental part of the current work was performed in the laboratory of Nevada Nanotech Systems, Inc. (NNTS).

Figure 1 shows the basic experimental setup for collecting sensory data during exposure of the microcantilever sensor array to the gaseous mixture containing an analyte.

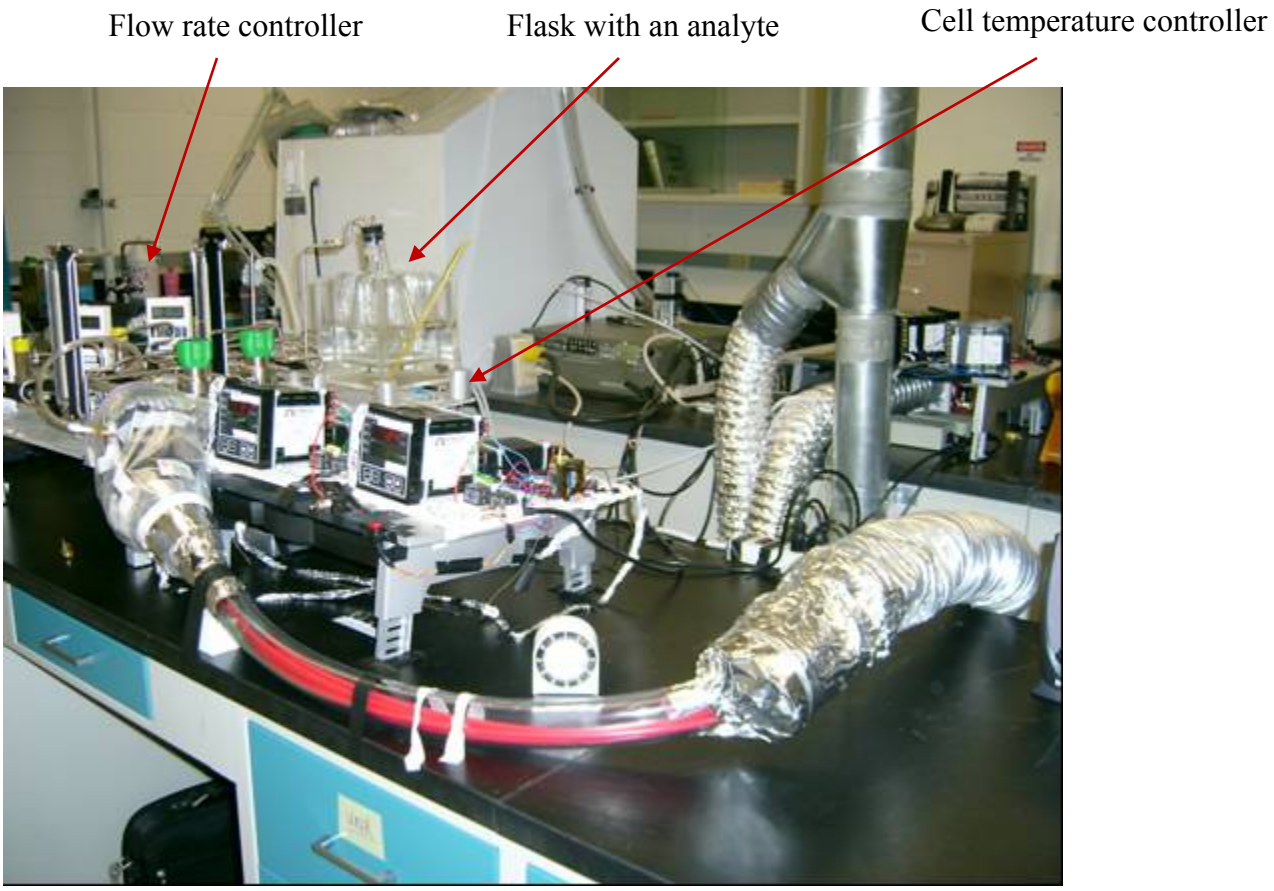

Figure 1. Basic experimental setup.

The flow rate control system allows us to create and maintain the desirable concentration of an analyte in the gaseous mixture (Figure 1, Figure 2) that the microcantilever sensor array (Figure 4) has to be exposed to. The dry air was forced to flow under excess pressure through a flask with an organic solvent (the chemical analyte) and the gaseous mixture of the dry air highly saturated with vapors of the given analyte was subsequently diluted several times until the needed concentration of an analyte in the air was reached.

Figure 2. Flow rate control system for controlling the desired concentration of the chemical vapors.

During the experiments some heating of the microcantilever array cell was applied as well. For heating (Figure 3), a different amount of electrical current was applied to the entire array of the cantilevers (all microcantilever sensors were heated and cooled simultaneously)

Figure 3. Temperature adjustment box for controlling the temperature of the array cell.

For the current work, we used a new generation array chip, called M10, for collection all data for our experiments (Figure 4).

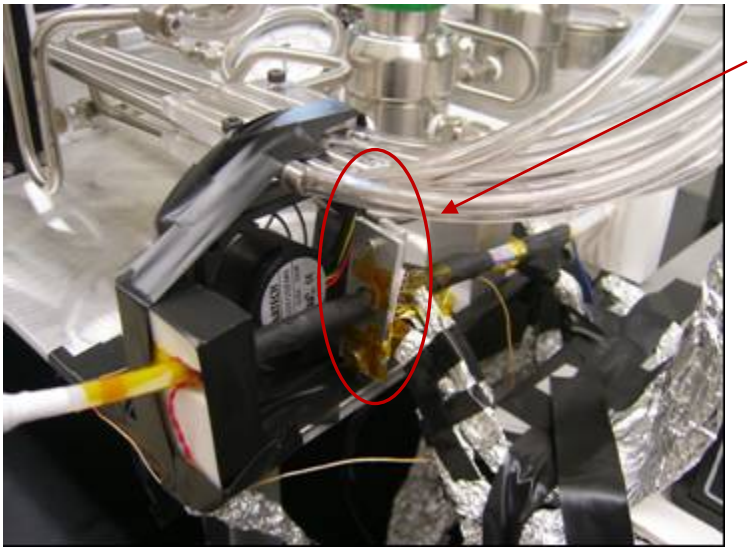

Figure 4. The location of the M10 cantilever array within the system.

Theoretically, this array has a large number of cantilevers, but only one row of them (ten cantilevers total) was wire-bonded and seven out of these ten cantilevers were coated with seven different coating materials. The remaining cantilevers were left uncoated.

The polymers that were used for coating the cantilevers and their respective chemical properties are:

- OV275 dipolar, moderately basic polymer
- PDMAEMC strong basic polymer
- PBM dipolar, basic polymer
- PDPZ polarizable polymer, contains phenyl groups
- PECH moderate dipolar polymer, contains moderate hydrogen-bonds
- PDMS nonpolar polymer
- BSP3 strong hydrogen-bond acidic polymer

All cantilevers in the array are driven into oscillation by an external circuitry and the resulting resonance frequencies were recorded. Figure 5 shows a snapshot of a graphical representation of resonance frequencies of all ten cantilever sensors in the array on an acquisition software application screen. The acquisition software application was tuned in such a way that seven different windows with all ten resonance frequencies (from all wired cantilevers) were set for monitoring gathered resonance frequency data simultaneously on the same screen:

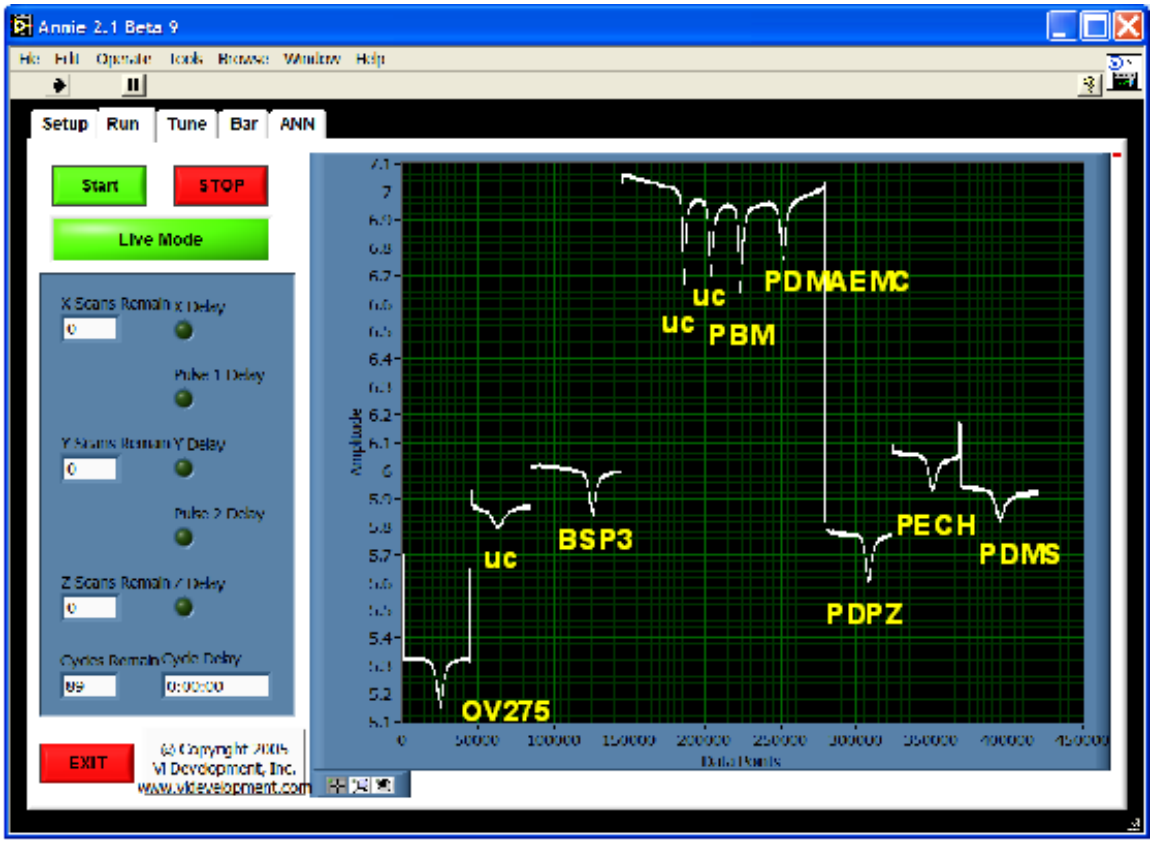

Figure 5. The figure shows a snapshot of all ten resonance frequencies: window 1 – OV275, span 45 kHz; window 2 – uncoated cantilever, span 40 kHz; window 3 – BSP3, span 60 kHz; window 4 – uncoated, uncoated, PBM, PDMAEMC, span 135 kHz; window 5 – PDPZ, span 45 kHz; window 6 – PECH, span 45 kHz; window 7 – PDMS, span 50 kHz.

3.2 Experiment Protocol Description

To calibrate our system, we ran a series of temperature experiments. The data were collected at five different temperatures: room temperature, 24, 28, 32, and 36°C (the thermo caps were set at the front and at the back of the array cell, so the temperature was measured with high precision).

In order to control the temperature during the experiment, special hardware consisting of a heater and fan was developed. The fan is automatically activated and the

heater is automatically set off if the temperature goes higher than desired; likewise, the heater is automatically set on and the fan is automatically set off if the temperature goes below the settings.

The objectives of the temperature experiments were the following:

- get stable and reproducible response of all cantilever at each temperature;
- make sure that the entire array is kept at designated temperature during the entire experiment (hardware issues);
- find the temperature–resonance frequency shift dependence for all cantilevers (so that we can use this information in the future to estimate how much the high temperature contributes to resonance frequency shifts of different cantilevers in some ambiguous situations).

This series of experiments resulted in the temperatures calibration curves shown in Figure 6:

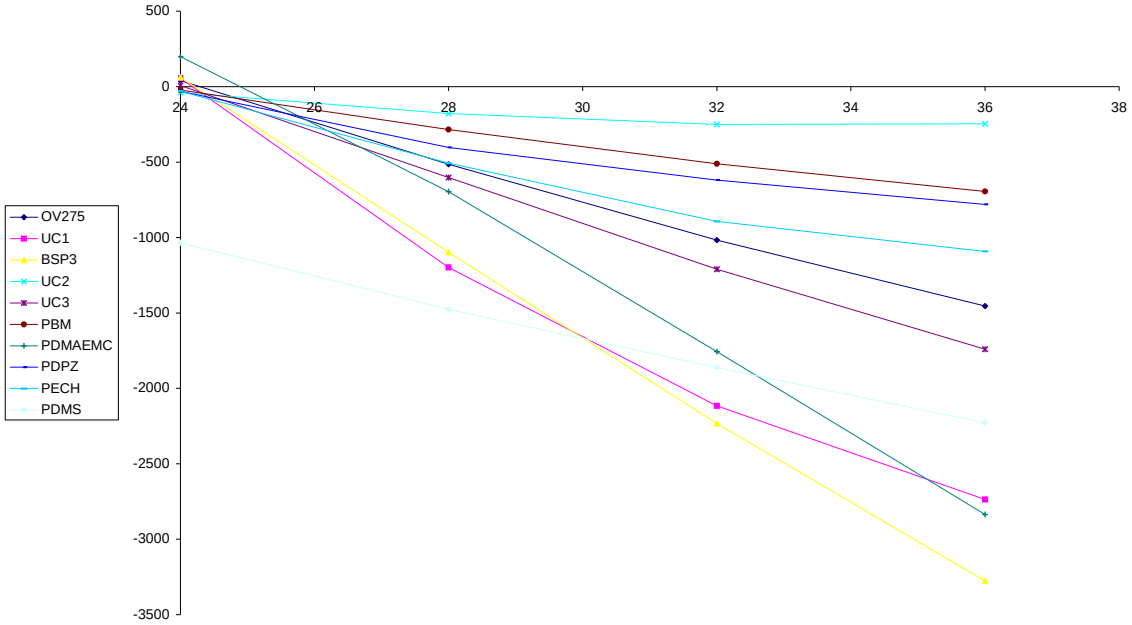

Figure 6. Temperature calibration curve (all cantilevers on the same graph).

Since all cantilevers demonstrated very good stability and all hardware issues were resolved, it has been decided to run our experiments at 24°C instead of room temperature. This choice insures a unified protocol for all experiments and overcomes the problem with so-called "ambient temperature" which is different not only during different seasons, but even during the same day and is very sensitive to many uncontrollable factors (such as an air conditioner, a room heater, the number of people around, an amount of different electric circuitries around, etc.).

After a series of experiments, the unified protocol described below was designed and implemented for automatic data collection by data acquisition software.

The base temperature of the array cell was 24°C. The flow rate of gaseous mixture was set to 400 ml/min. Each experimental run started with collecting data of dry air (at 24°C). The first 60 measurements were made with a rate approximately 2 scans per

minute; the remaining 240 measurements were taken without any delay (approximately 2 scans per second). Between the 11^{th} and 12^{th} scans, the chemical vapors were introduced into the gaseous mixture (we used only three different concentrations of the chemical vapors: 7%, 18%, and 26%). Approximately 40-42 measurements were taken at very high temperature (the electrical impulse was applied to cantilevers between scans 121-123 and 164-166, estimated temperature was 100-150°C); after removing the heat, the remaining approximately 135 measurements were taken while the array was cooling to 24°C.

After a cycle of the experiment with the chemical vapors was over, the next cycle was a "refreshment run." During this refreshment run the protocol was almost the same except that halfway between the 11^{th} and 12^{th} scans the chemical vapor gaseous mixture was replaced by the dry air and the entire array was heated at 55°C to speed up the desorption process of the analyte molecules from the polymer layers (during the refreshment cycle data were collected as well).

The protocol of the experiments with chemical vapors was designed in such a way so that we collect as much versatile information as possible:

- how fast different cantilevers start reacting with the introducing of a specified concentration of the specified chemical vapors;
- how fast the cantilevers get into the "steady" state (the resonance frequency is not changing any more);
- what happens during heating, cooling down, etc.

Besides impedance and resonance frequency shifts, we also measured the peak heights of each frequency during each scan (we assumed that it might be a valuable feature as well for our feature vectors).

Another positive characteristic of the above protocol was that the data did not depend on the baseline information, which might be recorded under slightly different conditions every time it was needed. In our experiments, we used the very first scan in each run as a baseline for the remaining 299 scans. By doing so, we measured only the relative changes during *each* experiment (we didn't have an impact of a so-called "accumulation" factor, when the baseline was getting further and further from the current plot, since the array never had a chance to be completely refreshed during the entire day of the experiments and it didn't completely release everything it accumulated during each run).

3.3 Data Collection Results

For the current work, we conducted experiments using vapors of different concentration (7%, 18% and 26%) of three different chemicals: acetone, toluene and ethanol. Figure 7 – Figure 12 show the responses of the cantilever array from some of these experiments.

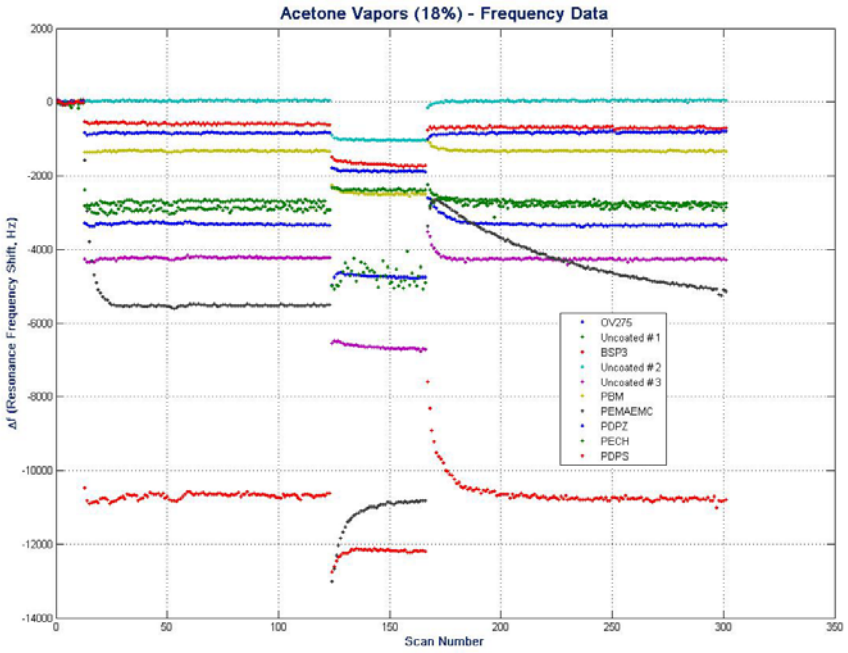

Figure 7. Resonance frequency shifts of all cantilevers during exposure of the array to 18% of acetone.

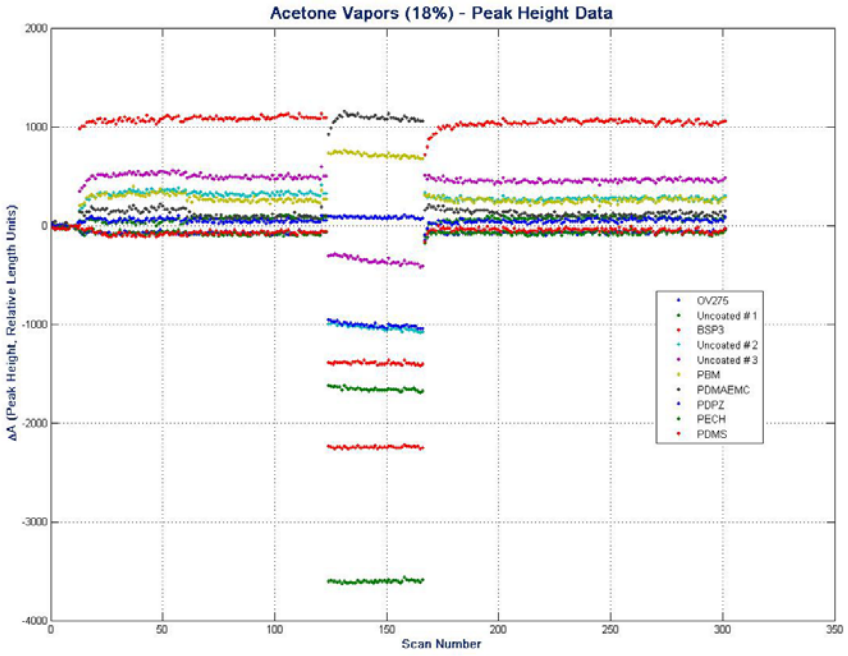

Figure 8. Heights of resonance frequency peaks of all cantilevers during exposure of the array to 18% of acetone.

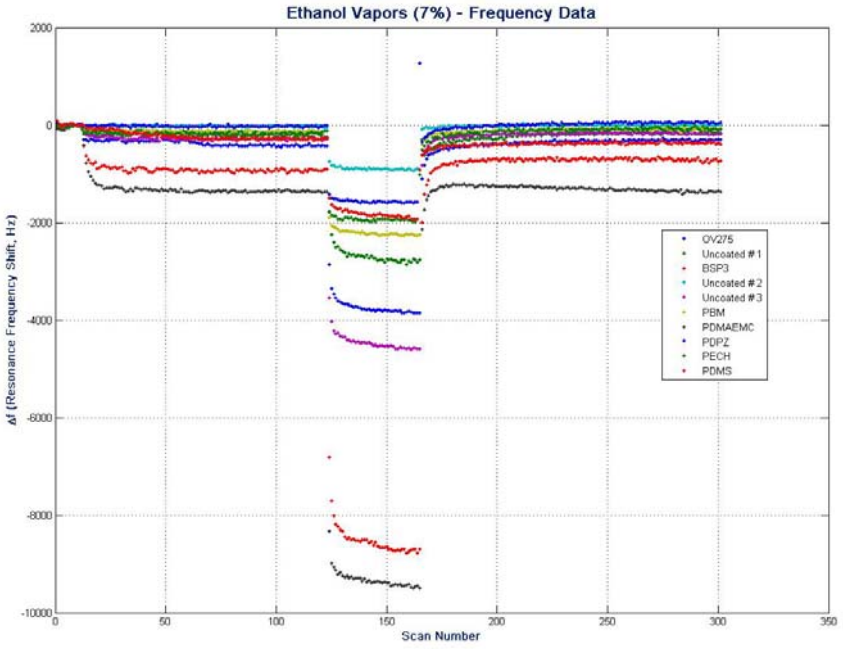

Figure 9. Resonance frequency shifts of all cantilevers during exposure of the array to 7% of ethanol.

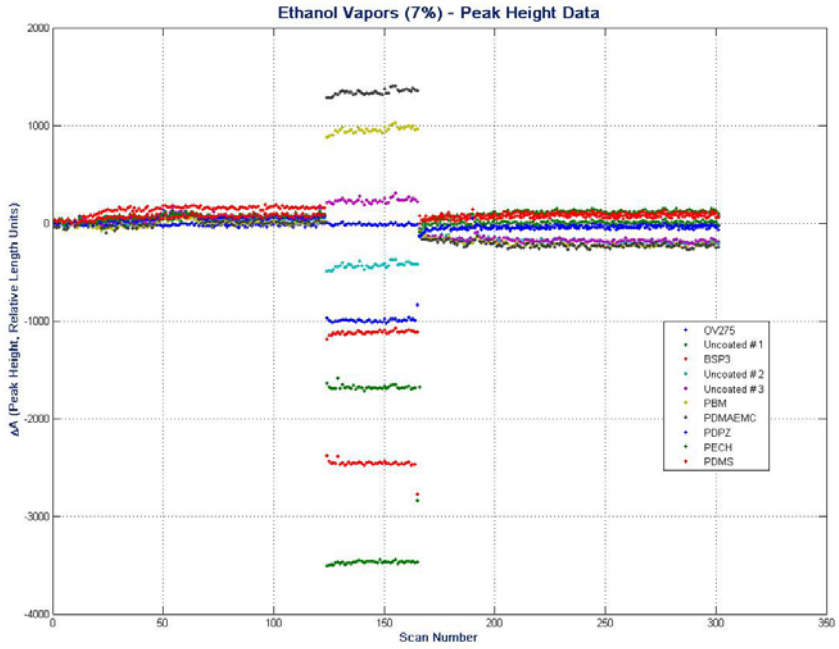

Figure 10. Heights of resonance frequency peaks of all cantilevers during exposure of the array to 7% of ethanol.

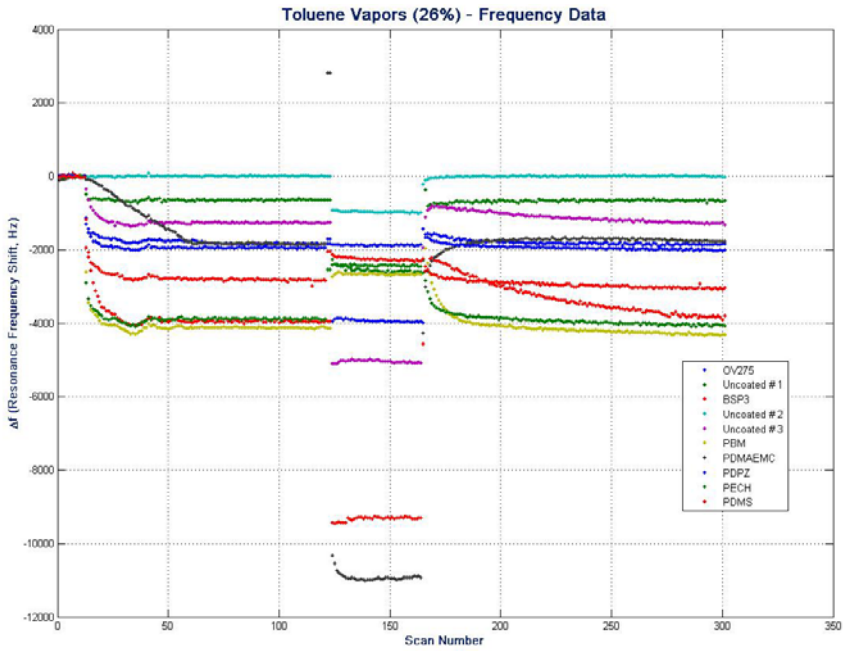

Figure 11. Resonance frequency shifts of all cantilevers during exposure of the array to 26% of toluene.

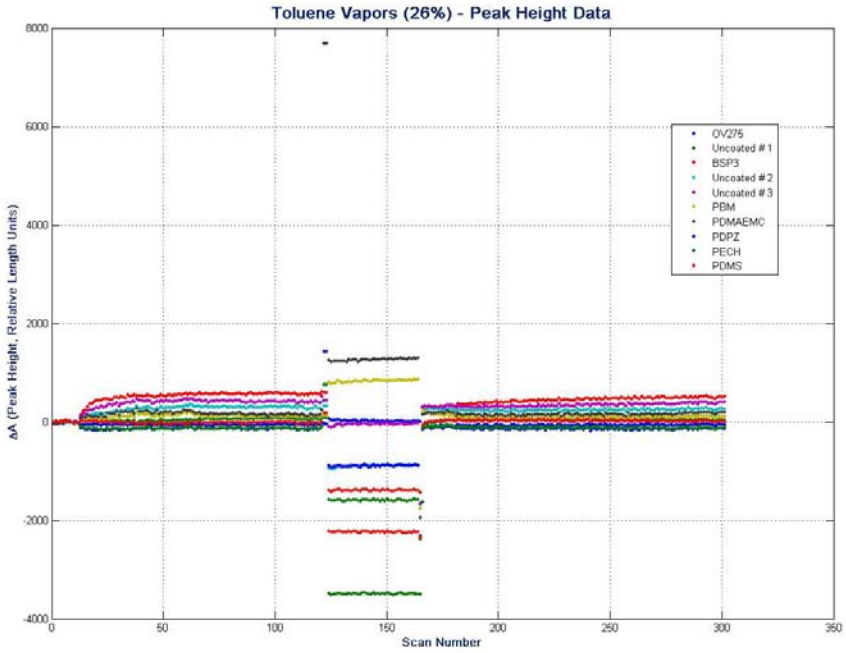

Figure 12. Heights of resonance frequency peaks of all cantilevers during exposure of the array to 26% of toluene.

3.4 Feature Extraction

While running the experiment, our system takes different measurements according to the protocol described above (such as resonance frequency, impedance) and saves them into an output file. After processing this file using a peak finding routine (this program was created by Dr. Jesse Adams from NNTS), a file consisting of almost 7000 different measurements is created. For each cantilever there are 300 values of the resonance frequency shifts measured at specified time points, 300 values for the peak heights of each resonance frequency peak, and the rest of the data is impedance information, which has been measured in several chosen points along the baseline of several cantilevers.

In order to reduce the amount of information to be processed, we extracted a subset of values from the total of 7000 pieces of data by applying our knowledge of the input domain (will be explained shortly), which helps create a feature vector that fully characterizes the gaseous mixture along with the conditions of the experiment.

In the current work we used data recorded for the following cantilevers: cantilevers coated with OV275, BSP3, uncoated cantilever # 3, cantilevers coated with PBM, PDPZ, PECH, and PDMS. Thus, we used the information obtained by only seven out of ten cantilevers. We left out the data collected by the cantilever coated with PDMAEMC and the remaining two out of three uncoated cantilevers, because these three sensors provided very inconsistent information. Possibly, that could be due to some physical defects of these three cantilevers, such as some foreign body like a piece of fiber lying on the sensor, or in the case of PDMAEMC, the uneven coating or the unknown

properties of this polymer that easily accumulates but not so easily releases the molecules of certain chemicals.

Figure 13 – Figure 15 illustrate the strategy that we used to extract the most prominent features from the resonance frequency responses of the cantilever sensors in the array.

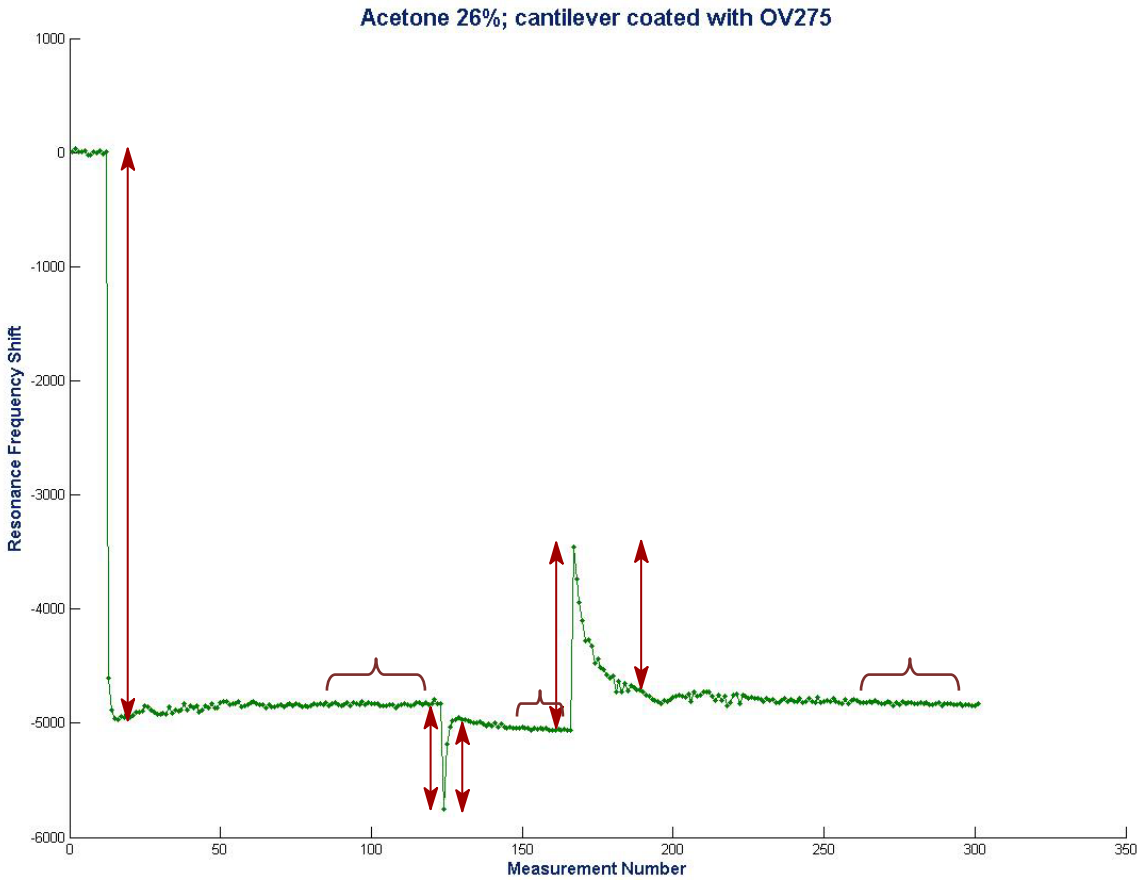

Figure 13. The figure shows the measurements for resonance frequency of the cantilever coated with OV275 polymer taken according to the protocol (described above). Red bidirectional arrows represent the difference taken before and after some conditions were changed, red curly braces indicate the areas on the graph where the row data as an average over 10-20 points were used.

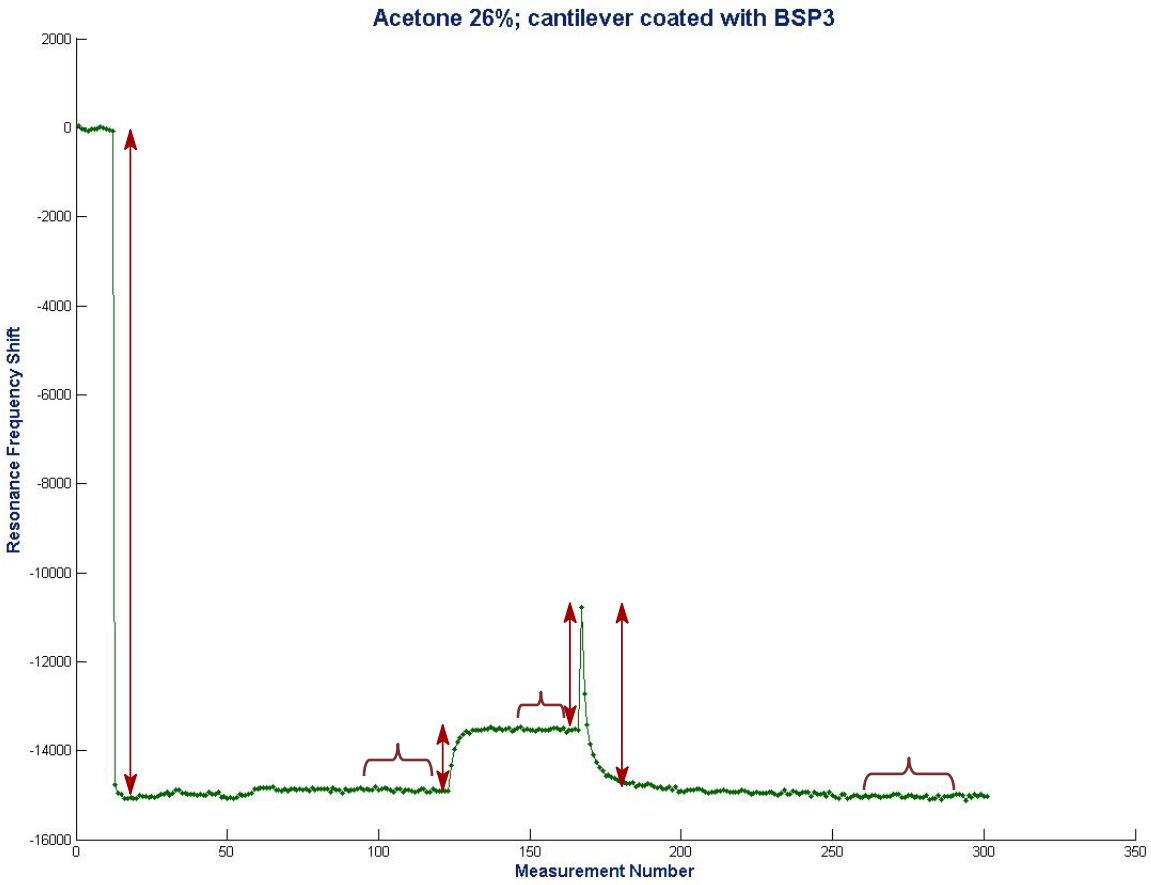

Figure 14. The figure shows the measurements for resonance frequency of the cantilever coated with BSP3 polymer taken according to our protocol. Red bidirectional arrows represent the difference taken before and after some conditions were changed, red curly braces indicate the areas on the graph where the row data as an average over 10-20 points were used.

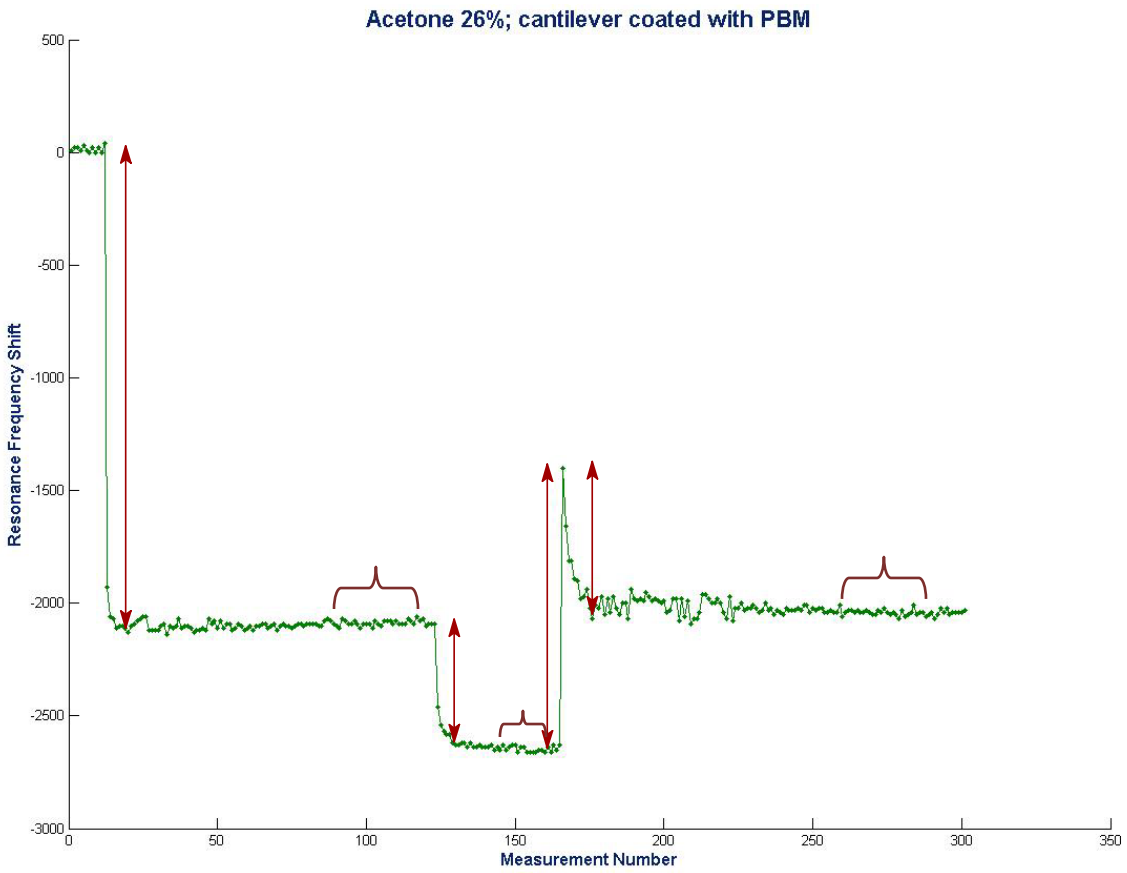

Figure 15. The figure shows the measurements for resonance frequency of the cantilever coated with PBM polymer taken according to our protocol. Red bidirectional arrows represent the difference taken before and after some conditions were changed, red curly braces indicate the areas on the graph where the row data as an average over 10-20 points were used.

By extracting the features for our exemplar data vectors in the fashion shown above, we created a data set consisting of feature vectors with 49 different features. However, during the early stage of testing the pattern recognition algorithms on the given sensory data we realized that some of the extracted features had not been consistent throughout the entire experimental data set. After thorough consideration, 15 out 49 features had been removed and 34-dimensional feature vectors were used for the further testing.

We also made several attempts to include more features in our vectors, such as polynomial coefficients given by a curve fitting procedure and height values of resonance frequency peaks. As we can see from the provided graphs, there are some areas that correspond to changing the temperature of the array cell (points 123-130, 165-175 – both parts of the curves fit nicely into polynomial of degree 3) or to introducing the chemical vapors in the air (points 12-20 – this part of the graph fits into polynomial of degree 2) that could be used as features in our feature vectors. We hoped that by adding more unique features to the feature vectors, we might significantly improve the classification accuracy of our algorithms. However, it turned out that those features (polynomial coefficients and peak heights) were inconsistent and unreliable from the experiment to experiment and instead of adding the additional distinctive characteristic, those features added more ambiguity and uncertainty.

In the end we kept the features that most closely described a variety of states that the cantilevers went through during the experimental run. Among the features we kept in our feature vectors were: 1) changes of the resonance frequency values after introducing an analyte into the air and after applying and removing the heat, and 2) the resonance frequency shifts of the cantilevers, averaged over several measurements during the steady states of the cantilever array before applying the heat, during the heating process, and at the end of the experiment when the array was cooled down to 24°C.

4 Theory and Algorithms Details

The ultimate goal of our research was to create a reliable algorithm that after training on a limited set of labeled feature vectors from various classes can recognize any unseen feature vector as belonging to one of these classes (or even more than one class, but with a different degree of confidence).

Therefore, we needed to create a reliable classifier system that could use a learning algorithm (or some combination of various learning algorithms) to gain enough knowledge about the problem domain to be able to correctly recognize any unseen sample afterwards. Thus, we had to successfully solve two separate problems: (1) to make our system learn from a limited pool of labeled pieces of data and (2) to teach our system to correctly label any number of new, unseen and therefore unlabeled samples from the same problem domain. Sometimes an algorithm includes solutions to both problems (learning and classification) at once; sometimes we have to seek different algorithms for each problem independently.

Machine learning and classification methods for pattern recognition are extremely versatile. Among them we can mention the most popular ones, such as Principal Component Analysis (PCA) [47], [48], and Multiple Discriminant Analysis (MDA) [49], probabilistic neural networks (PNNs) [50], [51], [52], [53], [54], radial basis function neural networks (RBFNNs) [55], [56], [57], [58], [59], crisp and fuzzy clustering [60], [61], [62], [63], [64], Support Vector Machines (SVMs) [65], [66], [67], [68], [69] and genetic algorithms (GAs) [70], [71], [72], [73], [74].

Below are some definitions and notations that will be used throughout the rest of this work.

A *feature vector* (pattern, object) $\vec{x}$ is a single data item in the data set under observation. Typically, it is a vector in the *N*-dimensional vector space $\Re^N$: $\vec{x} = (x_1, x_2, ..., x_N)$. Each individual scalar component x_i of vector $\vec{x}$ is called a *feature* (attribute, dimension, or variable). A data set of *Q* feature vectors is denoted $X = \{\vec{x}_1, \vec{x}_2, ..., \vec{x}_Q\}$ or $X = \{\vec{x}^{(q)} : q = 1,2,...,Q\}$, where the *q*-th feature vector in *X* is denoted $\vec{x}^{(q)} = (x_1^{(q)}, x_2^{(q)}, ..., x_N^{(q)})$. A *class* is a certain category of the objects (feature vectors) that has some unique or distinctive characteristics that easily distinguish it from other classes in the set. A feature vector can be *labeled*, meaning that we are provided with the information to which class the particular feature vector belongs, or *unlabeled*, meaning that we do not know this type of information.

The notion of a feature vector proximity measure is fundamental for all algorithms we used in the current research. We used the Euclidean distance as a measure of similarity between two feature vectors drawn from the same feature space:

$$d(\vec{x}^{(q)}, \vec{x}^{(r)}) = \sqrt{\sum_{i=0}^{N} \left(x_i^{(q)} - x_i^{(r)}\right)^2} = \| \vec{x}^{(q)} - \vec{x}^{(r)} \| \qquad (1)$$

In order to find the best possible solution to our problem of classifying specific sensory data, we implemented several learning and classification methods and tested them on a well-known benchmark data set, the Wisconsin Breast Cancer Database that contains 699 9-dimensional feature vectors (instances of two classes – malignant and benign) [75]. The feature vectors of the entire data set have been standardized

independently for each feature, so that they belong to the hypercube $[0,1]^N$ (N is dimension of the feature space), which permits each feature to have the same influence on the classifier systems. 7-Fold cross validation of the Wisconsin Breast Cancer Data Set has been used to tune the parameters and evaluate classification accuracy for all algorithms we used in the current work. Thus, this data set has been divided into seven training/testing set pairs (six pairs of sets containing 599 feature vectors in the training set and 100 feature vectors in the testing set and one pair of sets containing 600 feature vectors in the training set and 99 feature vectors in the testing set).

4.1 Extended Classifier System (XCS)

XCS, a recently developed classifier system in the context of Evolutionary Computing [74], bases its fitness function on classification accuracy and implements so-called reinforcement learning. XCS creates and maintains the population of classifiers, each of those classifiers maintains its own prediction of the expected reinforcement ("payoff," "reward") from the environment. XCS executes the genetic algorithm (GA) in the environmental niches defined by the match to the given input sent by the environment, instead of using random mating and mutation within the entire population of classifiers. As a result, XCS tends to evolve the classifiers that are not only highly accurate, but also are maximally general. By "general classifier," we mean a classifier that considers inputs that have the same consequences on the environment as identical. With this, a general classifier captures regularity in the environment and by incorporating "don't care" symbols is capable of matching more than one input vector. [76], [77].

There are several main aspects of XCS that should be emphasized.

First, XCS is a learning machine, that is, a learning program within a computer. Its behavior significantly improves over time through interaction with the environment that constantly sends feedback on XCS's performance.

Second, XCS learns *on-line*, meaning that it cannot collect a lot of experience in some temporary storage and then process all the collected information. Instead, it learns as it goes along – it extracts the implication of every single experience as it occurs.

Third, XCS tries to capture regularities of the environment. This means that XCS tries to create not only accurate classifiers, but also general ones. By generality of the classifier we mean that it holds the knowledge about some part of the problem space (not only about a single representative of that space) being maximally accurate at the same time. A machine with even a small number of sensors will encounter an enormous number of sensory states in any reasonably complicated environment. Thus, it is extremely important for the learning algorithm to be able to capture the similar behavior of the environment and group the states of the environment having the same implication for its behavior. Thus, generalization is a core of XCS. Because of generalization, XCS has an intrinsic tendency to evolve accurate, maximally general classifiers [77].

Furthermore, XCS learns to get reinforcements, in other words, it learn to act in such a way that it always receives maximally possible rewards from the environment. Often, it is very difficult to "explain" to the machine what it should do in order to achieve some goals that we set for it. Instead, it is much easier to establish the framework of reinforcement learning – every time the machine does something that we want we give it a reward. This way, we are leaving for the machine to figure out by itself what exactly it should do in order to be rewarded.

Thus, XCS acts as a reinforcement learning agent: it receives an input that describes the current state of the environment and reacts on the given input by emitting some actions, which are immediately sent back to the environment. This action can affect the environment and may result in some payoff. For this work, we restrict inputs from the environment to binary strings. The input space is denoted by $S \subseteq \{0,1\}^L$, where L is the length of the input string. XCS's knowledge is contained in a set of condition-action rules called *classifiers*. Each classifier consists of a condition part, an action part, and a prediction part. The *condition* $C \in \{0,1,\#\}^L$ specifies which input states $s \in S$ the classifier can match ("#" is a "don't care" symbol). The *action a* specifies the action that the classifier has chosen and expected a payoff. Classifier's *prediction p* can be defined as an average of the payoff received (internal or external, or some combination of both) when the classifier's action controls the system. Among other important XCS's attributes are the following: *prediction error* ε (an average of a measure of the error in the prediction parameter) and *fitness F*, which estimates the *accuracy* of the payoff prediction *p* (normally, *F* is some inverse function of the prediction error that basically represents the classifier's accuracy; therefore, the XCS's fitness calculation is entirely based on its classification accuracy).

Since there are many classifiers within the system at any time (perhaps, hundreds), after XCS has been trained for a while, it will contain the classifiers that accumulate the knowledge about all parts of the input and action space that it has experienced so far. This ability to accumulate the meaningful knowledge in some limited set of classifiers makes XCS unique compared to other types of learning machines. In

XCS, the knowledge about some chunk (could be very considerable) of the problem space is contained in individual classifiers (sometimes, even in only one of them). We can take a classifier out of the context of the entire system and learn a lot about some particular subspace of the problem space. In contrast, the knowledge about some problem in the neural network, for example, is distributed over the whole network, all its nodes and node's weights, and nothing in this network taken separately can tell us anything useful about the problem it has learned.

4.1.1 Performance of XCS

For the following discussion, we assume that the population [*P*] of the classifiers is not empty. XCS interacts with the environment as follows.

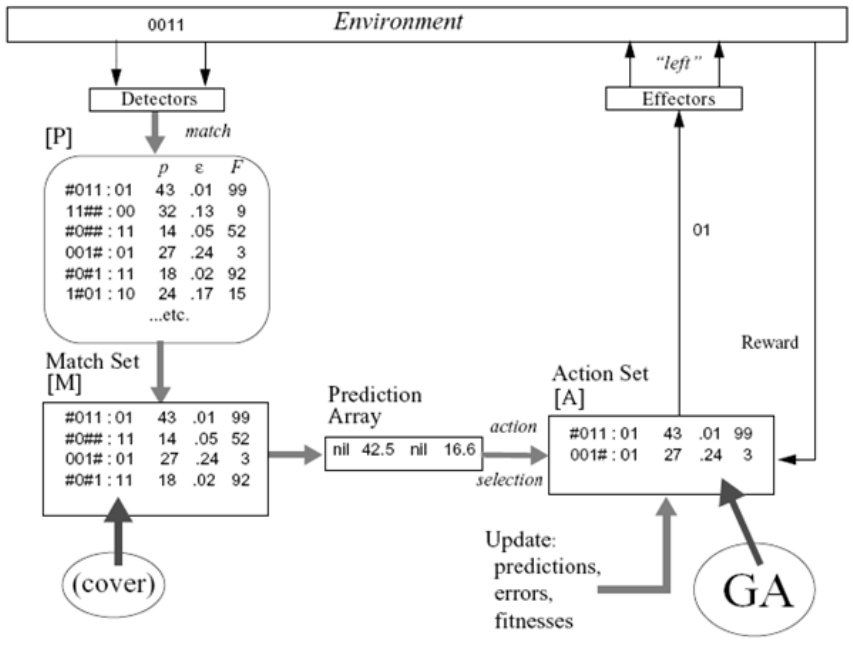

Figure 16. Schematic illustration of XCS's performance cycle (the scheme was taken from [74]).

When the system receives an input from the environment it forms a *match set* [*M*] of classifiers whose conditions are satisfied by the current input. If the match set is empty

or it contains less than some specified number θ_{mna} of classifiers with different actions, *covering* classifiers are created with a condition that matches the current input and some random action. Specifically, each attribute in the condition of a covering classifier is set to "#" with a probability $P_{\#}$ and to the corresponding input symbol, otherwise. For each action a_j in [M], XCS computes the *system prediction array* $P(a_j)$, which is an estimate of the payoff that the system expects when action a_j is performed. The prediction array is computed by the fitness-weighted average of all matching classifiers that specify action a_j.

XCS often selects an action with respect to the values in the prediction array. Even though it seems that XCS should always pick an action that has the highest prediction in the prediction array, XCS must sometimes choose apparently sub-optimal actions, in order to be sure that the apparently optimal classifiers are in fact optimal. This is an example of the *explore/exploit* dilemma. The system would like to choose the best action all the time in order to maximize the payoff, but it cannot determine the best action without sampling other actions as well. The system may simply pick the action with the largest prediction (deterministic action selection). Alternatively, the action may be selected probabilistically, with the probability of selection proportional to $P(a_i)$ (roulette-wheel action selection). In some cases the action may be selected completely at random (from actions with non-null predictions).

In the current work, we have implemented an advanced scheme of action selection – the gradient change of the explore/exploit rate during the training phase. For this purpose, the entire training set was divided into four (uneven) partitions so that the different explore/exploit rates could be applied to meet the needs of the classifier system

(e.g., at the beginning of the training phase, when there are none of experienced classifiers, the higher explore rate should be used, and so on). Exploration experience (EE) parameter also could be viewed as the number of inputs from the training set processed so far.

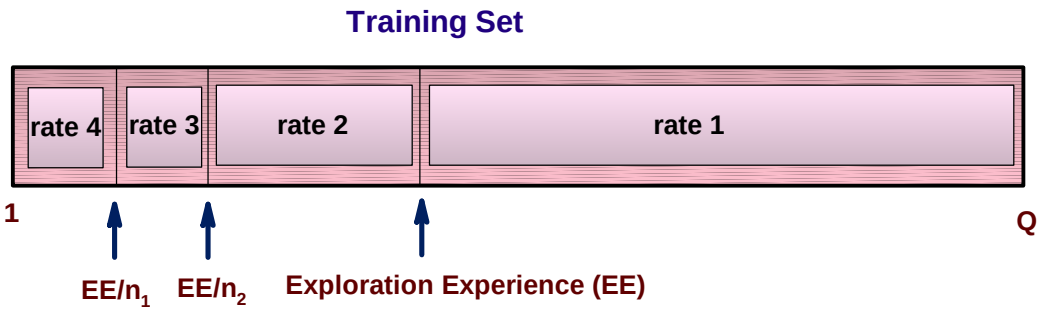

Figure 17. New flexible scheme for action selection that can be finely adjusted to each specific problem space.

Once the action is selected, the system forms an *action set* [A] consisting of the classifiers in [M] advocating the chosen action. An immediate reward *R* may (or may not) be returned by the environment.

4.1.2 Reinforcement Component

XCS's reinforcement component consists in updating the *p* (*prediction*), ε (*prediction error*), and *F* (*fitness*) parameters of classifiers once the reward *R* is obtained from the environment.

In the literature, there are a lot of discrepancies and confusion about how exactly (and in what order) all the classifier's parameters should be updated. We had performed several experiments that vary the order of the updates, and some different schemes of calculating the updated parameters and came up with the solution that we think is the best. The following approach in executing the reinforcement component of XCS has been

established and confirmed by the experiments (our scheme mostly agrees with the order of updates listed in [77]; but in contrast we update the parameters of those classifiers, which have not been tested a particular number of times, differently compare to the conventional way):

1. The current *prediction error* is calculated:

$$\varepsilon_j = | P - p_j | \qquad (2)$$

where ε_j is a prediction error of the *j*-th classifier, *P* is a payoff from the environment, p_j is a prediction of *j*-th classifier.

2. The *prediction error* is updated based on the classifier experience (the number of time the classifier has been selected to be in [*A*]). If its experience is less than some specified threshold, then ε_j is an average of all previous values of this classifier's prediction errors and the current one. Otherwise:

$$\varepsilon_j \leftarrow \varepsilon_j + \beta \times (| P - p_j | - \varepsilon_j) \qquad (3)$$

where $\beta (0 < \beta < 1)$ is the learning rate.

3. Classifier's *accuracy* k_j is computed. There are several popular functions for computing classifier's accuracy. We had tried the following three functions in our experiments:

(a) $k_j = \alpha \times \left(\frac{\varepsilon_j}{\varepsilon_0} \right)^{-\nu}$ (4)

if $\varepsilon_j > \varepsilon_0$

otherwise, $k_j = 1$

(b) $k_j = \exp\left[\ln\alpha \times \left(\frac{\varepsilon_j - \varepsilon_0}{\varepsilon_0}\right)\right]$, if $\varepsilon_j > \varepsilon_0$

otherwise, $k_j = 1$

(c) $k_j = \varepsilon_j^{-\nu}$, if $\varepsilon_j > \varepsilon_0$

$k_j = \varepsilon_0^{-\nu}$, otherwise

where α ($0 < \alpha < 1$), ε_0, and ν ($\nu \approx 5$) are special constants set by the programmer. From our tests, we observed that function (a) outperformed the other two. Thus, we successfully used that function (Eq. 4) in our implementation.

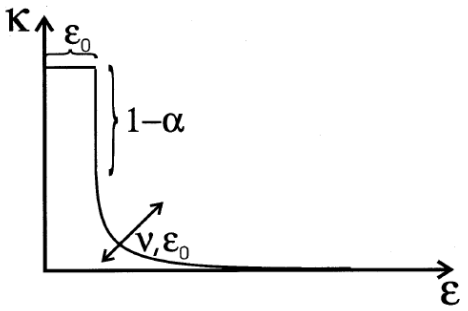

Figure 18. The classifier's accuracy as a function of the classifier prediction error ε_j (Eq. 4) (the graph was taken from [77]).

4. The classifier's *relative accuracy* is computed for each classifier by dividing its accuracy by the total accuracies in the set [*A*]:

$$k_j' = \frac{k_j}{\sum_i k_i} \qquad (5)$$

5. The relative accuracy is used to adjust the classifier's *fitness* F_j. Fitness is updated differently based on classifier's experience in [*A*]. If this classifier has been adjusted

for a specified number of times (i.e., its experience exceeds the threshold value), then:

$$F_j \leftarrow F_j + \beta \times (k_j^{'} - F_j) \qquad (6)$$

Otherwise, F_j is set to the average of the current and previous values of $k_j^{'}$.

6. *Prediction* itself is updated (again, based on classifier's experience); if the classifier is not experienced enough, p_j is calculated as an average of all previous values of this classifier's prediction and the current one. Otherwise:

$$p_j \leftarrow p_j + \beta \times (P - p_j) \qquad (7)$$

where $\beta (0 < \beta < 1)$ is the learning rate.

The idea behind the accuracy calculation is visualized in Figure 18: ε_0 is a threshold measuring the extent to which errors are accepted, α causes a strong distinction between accurate and not quite accurate classifiers, and the steepness of the succeeding slope is influenced by ν, as well as ε_0. Thus, in XCS the classifier fitness is an estimate of the classifier's accuracy relative to other classifiers and behaves inverse proportional to the reward prediction error. Errors below the threshold are regarded as having equal accuracy.

4.1.3 Discovery Component

From time to time (not always!) a genetic algorithm (GA) is applied to the classifiers in the current action set [*A*]. From the beginning, XCS performs the GA in a niche (first introduced by Booker in 1982 [78]), and it does not use the entire population of classifiers as many other classifier systems do. The basic idea of a niche GA instead of

using the entire population is that it eliminates the undesirable competition that otherwise occurs between classifiers in different match sets. In addition, crossovers within a niche are more likely to yield useful classifiers than crossovers between potentially unrelated classifiers that match in different niches.

The GA selects two parental classifiers with probability proportional to their fitness; two children are generated by reproducing, crossing, and mutating the parents. In the current implementation of XCS, we used a simple single-point crossover and two types of mutation: *free mutation* [74] and *niche mutation* [79]. In free mutation, each bit of the classifier condition is mutated to the other two possibilities with equal probability. In niche mutation, a classifier condition is mutated so that it still matches the current input, i.e., a don't-care symbol is mutated to the corresponding input value, while 0 or 1 is mutated to don't-care. Niche mutation generally results in a faster convergence time, whereas free mutation causes broader exploratory behavior, faster knowledge transfer and, thus, higher robustness. In the current work, we have added one feature to the free mutation implementation. While testing our implementation, we have noticed that the system often chooses the very accurate classifiers with a wrong action. To address this issue, we have modified free mutation in such a way that action is allowed (with some small probability) be mutated as well. Thus, in the current work, when performing free mutation, the system can choose from the pool of all available actions, except the one that the classifier currently posses.

After new classifiers have been created by the GA, they are inserted into the population [*P*]. As happens in all the other models of classifier systems, parents stay in the population competing with their offspring.

4.1.4 Deletion Schemes

Since XCS maintains the size of its population of classifiers constant, every time new classifiers have to be added to the population [*P*], XCS faces a problem of deletion. The importance of deletion in XCS used to be underestimated considerably. If in a standard GA a chromosome can be evaluated (assigned a reasonable fitness value) immediately, in XCS, however, a chromosome can only be fully evaluated after many interactions with the environment (when a classifier has considerable experience of being in [*A*]).

Because a new classifier must normally be tested on many trials before XCS can be certain of its fitness, it is a good idea to set its initial fitness to a low default value and increase it slightly each time it proves itself useful. This way accurate classifiers gradually increase their chances of participating in reproduction. Bad classifiers (i.e., classifiers that are inaccurate or have low accuracy) tend not to increase in fitness and so tend not to participate in reproduction.

But since all classifiers initially have a low fitness, a bias against low fitness classifiers is also a bias against new classifiers, both good and bad (accurate and not). The stronger the bias, the more the system will tend to delete useful new classifiers before it has the possibility to test them and evaluate how good they are.

To address this problem, we used the advanced deletion approach proposed by Kovacs in 1999 [80]. This approach considers the probability of deletion of each classifier to be proportional to the estimate of size [*A*] (one more parameter that each classifier updates every time it gets into [*A*]) until a classifier has been used on some specified number of trials. After that, the probability of deletion of each classifier is

multiplied by the mean fitness over the current population set [*P*] and is divided by the classifier's fitness if and only if its fitness is less than a small fraction δ (specified by a programmer) of the population mean fitness. This scheme helps to maintain approximately the same number of classifiers in each niche and to eliminate inaccurate classifiers that proved to be bad through numerous interactions with the environment. In addition to using this advanced scheme of deletion in our work, we have added one additional feature to protect inexperienced classifiers from deletion before they have been given a chance to be evaluated; which is to start the processing XCS with a fraction of maximally possible population of classifiers (100 or 200 out of 500, for example).

The presence in the population of accurate, but unnecessarily specialized classifiers is an undesirable feature of the classifier system. To address this problem, a so-called *subsumption deletion* scheme has been implemented in the current work as well. The approach can be describes as follows: every time a new classifier is created (by either the GA or by covering), the entire population is scanned to see if there exists a classifier whose condition logically subsumes the condition of the new classifier, has the same action and at least the same accuracy. If the test is satisfied, the new classifier is not injected into the population, but the *numerosity* (another important parameter of the classifier) of the classifier that subsumed that is incremented by one.

In order to implement *subsumption deletion*, we always insert the most general classifier into the population [*P*] first. This approach guarantees that less general classifiers would be subsumed during the insertion into [*P*] if the possibility arises.

The mention of numerosity parameter brings another important feature of XCS into light – the notion of *macroclassifiers*.

4.1.5 Macroclassifiers

In XCS, a *macroclassifier* technique is used to speed processing of matching [*P*] against the input vector and provides a clearer and more unambiguous view of population contents. Macroclassifiers represent a set of classifiers with the same condition and the same action by means of the *numerosity* parameter mentioned above. Thanks to the use of macroclassifiers, the resulting population [*P*] consists entirely of structurally unique classifiers, each with numerosity greater than or equal to 1. If a classifier is chosen for deletion, its numerosity is decremented by 1, unless the result would be 0, in which case the classifier is removed from [*P*].

In order to be sure that the system still behaves as though it consists of *N* regular classifiers, the functions are written so as to be sensitive to the numerosities, if that is relevant. For example, in calculating the relative accuracy, the probability of to be deleted or selected for mating, and so on, a macroclassifier with numerosity *n* will be treated as though it represents *n* separate classifiers.

Thus, the population as a whole is always treated as though it contains *N* regular classifiers, though the actual number of macroclassifiers in [*P*] may be substantially less than *N*, which gives a significant computational advantage.

4.1.6 Test Results

Implementation details of the current algorithm are given in Appendix A.

Since XCS intensively uses the random generated numbers, we run each test using 30 different seeds to randomize the `srand()` function. Therefore, each result has been obtained by 210 program runs (7-fold cross validation by using 30 different seeds).

For all tests in each category we used the same set of parameters that have been optimized in the previous testing procedures. For each test we used the same set of seeds:

$$\texttt{for } i = 0 \texttt{ to } i = 29$$

$$seed_i = 111 \times i + 17 \times i$$

In order to prove the benefits of our advanced gradient exploration rate scheme, we performed tests using different constant exploration rates first and then we run a series of tests that uses our gradient exploration rate scheme. Although these are just preliminary results and the parameters for the gradient exploration rate scheme could be adjusted even better, we can see that the average result for the best values of classification accuracy has been improved.

Table 1. Results of classification accuracy obtained by using the constant exploration rate.

PARAMETERS: constant exploration rate	Classification Accuracy (%)	
	average of max values for each set of tests (over 30 runs)	average over 210 program runs
"Choosing the action randomly" option is turned off	90.171	77.397
2	92.026	81.871
4	92.134	79.702
10	90.749	78.671
15	92.294	78.110
20	92.264	77.920

Table 2. Adjusting gradient exploration rate scheme (see Figure 17).

PARAMETERS: explore rate (gradient) EE; rate1; rate2; rate3; rate4	Partition of Training Set	Classification Accuracy (%)	
		average of max values for each set of tests (over 30 runs)	average over 210 program runs
200; 20; 10; 5; 2	1-1/4×EE (rate4); 1/4×EE-1/2×EE (rate3); 1/2×EE-EE (rate2); EE-Q (rate1)	92.266	77.887
400; 20; 10; 5; 2	1-1/4×EE (rate4); 1/4×EE-1/2×EE (rate3); 1/2×EE-EE (rate2); EE-Q (rate1)	92.266	77.830

600; 20; 10; 5; 2	1-1/4×EE (rate4); 1/4×EE-1/2×EE (rate3); 1/2×EE-EE (rate2); EE-Q (rate1)	92.266	77.992
600; 50; 10; 5; 2	1-1/4×EE (rate4); 1/4×EE-1/2×EE (rate3); 1/2×EE-EE (rate2); EE-Q (rate1)	92.635	76.804
600; 50; 5; 4; 2	1-1/4×EE (rate4); 1/4×EE-1/2×EE (rate3); 1/2×EE-EE (rate2); EE-Q (rate1)	92.635	76.813
600; 50; 5; 4; 3	1-1/10×EE (rate4); 1/10×EE-1/5×EE (rate3); 1/5×EE-EE (rate2); EE-Q (rate1)	92.635	76.837
1200; 50; 5; 2; 1	1-1/10×EE (rate4); 1/10×EE-1/2×EE (rate3); 1/2×EE-EE (rate2); EE-Q (rate1)	92.635	76.737
600; 50; 5; 2; 1	1-1/8×EE (rate4); 1/8×EE-7/8×EE (rate3); 7/8×EE-EE (rate2); EE-Q (rate1)	92.635	76.823
600; 50; 5; 2; 5	1-1/8×EE (rate4); 1/8×EE-7/8×EE (rate3); 7/8×EE-EE (rate2); EE-Q (rate1)	92.810	77.342

The next set of tests was created to adjust the niche mutation rate and demonstrate that allowing the action to be mutated as well during execution of the free mutation algorithm improves the results of classification accuracy.

Table 3. Results of classification accuracy obtained for different niche mutation rates.

PARAMETERS: niche mutation (NM) rate (probability of mutation = 4%; action mutation is ON)	Classification Accuracy (%)	
	average of max values for each set of tests (over 30 runs)	average over 210 program runs
NM OFF	89.553	78.365
NM = 2	91.866	77.863
NM = 4	90.540	77.298
NM = 8	92.635	76.813

Table 4. Results for classification accuracy with and without action mutation.

PARAMETERS: (niche mutation (NM) rate = 8) probability of mutation (%); action mutation (ON/OFF)	Classification Accuracy (%)	
	average of max values for each seed (over 30 runs)	average over 210 program runs
2; OFF	89.980	77.082
2; ON	91.312	79.764
8; OFF	91.495	75.596
8; ON	92.635	76.813

Finally, we run a set of tests to experiment with different deletion schemes and demonstrate an advantage of the scheme we have been using in our implementation of XCS. Thus, Deletion Scheme 1 refers to having the probability of deletion of each classifier be proportional to the estimate of size [*A*]; Deletion Scheme 2 refers to having the probability of deletion of each classifier be as in Deletion Scheme 1 and multiplied by the mean fitness over the current population set [*P*] and divided by the classifier's fitness; and Deletion Scheme 3 refers to the combination of the previous two that could be adjusted using the *deletion experience* (*DE*) parameter and using a fraction of maximum population size as an initial population of classifiers. In addition, to enhance the advantage of the advanced deletion scheme listed above, we also implemented and used subsumption deletion (see the description of XCS algorithm).

Table 5. Results of classification accuracy for different deletion schemes.

PARAMETERS: Deletion Scheme; Initial Population Size (Deletion Experience= 15)	Classification Accuracy (%)	
	average of max values for each seed (over 30 runs)	average over 210 program runs
1; 500	77.965	68.408
2; 500	79.110	68.939
3; 500	78.226	68.585
3; 300	87.048	73.101
3; 100	92.635	76.813

4.2 Kernel-Based Pattern Recognition Methods

After the noticeable success of Support Vector Machines (SVMs), a classification algorithm, that was introduced in 1995 by Vapnic [65] and which performs better than other classification algorithms in a wide range of problems, the usage of kernel methods has been extended into other areas of machine learning and pattern recognition as well: Kernel Fisher discriminant (KFD) [81], [82], kernel principal component analysis (KPCA) [83], and most recently, kernel-based hard and fuzzy clustering [84], [85], [86], [87].

The philosophy behind the versatile family of kernel methods is that the *kernel functions*, or just *kernels*, implicitly define nonlinear transformations that map linearly inseparable input data from the original input space $\Re^N$ into a higher dimensional *feature space F*, where the relations among the feature vectors can be represented in a linear form, and therefore, the data can be linearly separated.

Kernels are a special type of mathematical functions with specific properties. Each kernel $k(\cdot)$ computes the inner product of the images of the two data points in *F* and can be expressed as follows:

$$k(\vec{x},\vec{y}) = \Phi(\vec{x}) \cdot \Phi(\vec{y}) =< \Phi(\vec{x}), \Phi(\vec{y}) > \qquad (8)$$

where $\Phi : \Re^N \rightarrow F$ performs a mapping from the original input space $\Re^N$ into the feature space *F*, such that the image of any feature vector $\vec{x}$ in the feature space *F* becomes $\Phi(\vec{x})$.

The important aspect of this kind of nonlinear mapping is that it is possible to compute Euclidean distance in the feature *F* without even knowing Φ explicitly through the distance kernel trick [67], [88]:

$$\begin{aligned} \| \Phi(\vec{x}) - \Phi(\vec{y}) \|^2 &= (\Phi(\vec{x}) - \Phi(\vec{y})) \cdot (\Phi(\vec{x}) - \Phi(\vec{y})) \\ &= \Phi(\vec{x}) \cdot \Phi(\vec{x}) - 2\Phi(\vec{x}) \cdot \Phi(\vec{y}) + \Phi(\vec{y}) \cdot \Phi(\vec{y}) \\ &= k(\vec{x}, \vec{x}) + k(\vec{y}, \vec{y}) - 2k(\vec{x}, \vec{y}) \end{aligned} \qquad (9)$$

Examples of the mostly often-used kernels are:

Linear kernel:

$$k^{(l)}(\vec{x}, \vec{y}) = \vec{x} \cdot \vec{y} \qquad (10)$$

Polynomial kernel of degree *p*:

$$k^{(p)}(\vec{x}, \vec{y}) = (\alpha + \vec{x} \cdot \vec{y})^p, \qquad p \in \mathbb{N} \qquad (11)$$

Gaussian kernel:

$$k^{(g)}(\vec{x}, \vec{y}) = \exp\left(- \frac{\| \vec{x} - \vec{y} \|^2}{2\sigma^2} \right), \qquad \sigma \in \mathbb{R} \qquad (12)$$

Sigmoid kernel:

$$k^{(s)}(\vec{x}, \vec{y}) = \tanh(\alpha \times (\vec{x} \cdot \vec{y}) + \beta) \qquad (13)$$

In our work, we consistently used the Gaussian kernel, when it was applicable, as a kernel-induced metric for measuring distances between feature vectors or a feature vector and a center of a cluster in the feature space *F*. Gaussian functions have a long history of being used in machine learning and pattern recognition and proved themselves to be efficient and simple in computations and to be robust to noise and outliers in classification tasks.

Since the Gaussian kernel functions form the hidden units of a Radial Basis Function Network; therefore, they are often called the *RBF kernels*. For the Gaussian kernel the images of all feature vectors in *F* have norm 1, since $k(\vec{x},\vec{x}) = \exp(0) = 1$. The parameter σ controls the flexibility of the kernel. As the Gaussian kernel of two points becomes bigger, the closer those two points are in the input space.

Even though a kernel component of any kernel method is data specific, it can be combined with different algorithms to solve a wide range of tasks. Nowadays, more and more scientists and engineers, who are working in the different fields of machine learning and pattern recognition, embrace a new powerful paradigm of kernel methods and tend to view many traditional machine learning and pattern analysis algorithms from the standpoint of this new methodology. From this viewpoint, any algorithm that uses a kernel function to process the data and builds its discriminant function (also called a pattern function, which is used to process unseen examples in order to classify or label them) using kernels can be (and should be) considered as a kernel-based algorithm.

4.2.1 Radial Basis Function Neural Network (RBF NN)

Radial basis function neural networks (RBF NNs) are one of many powerful examples of kernel methods for pattern analysis. RBF NNs have been successfully used in a wide variety of applications and their learning and generalization abilities are well documented [55], [56], [57], [58], [59], [89], [90]. The architecture and training algorithms for RBF NNs are simple and their learning is considerably faster than other forms of multilayer neural networks.

Let $X = \{\vec{x}^{(1)},...,\vec{x}^{(Q)}\}$ be a training data set of Q labeled feature vectors, where each vector $\vec{x}^{(q)}$ is N-dimensional (that is, it has N features): $\vec{x}^{(q)} = (x_1^{(q)},...,x_N^{(q)})$. The architecture of the RBF NN can be presented as follows:

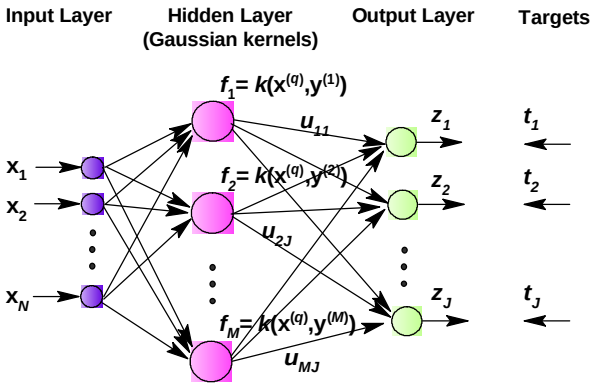

Figure 19. The radial basis function neural network (RBF NN) architecture.

The RBF NN has three layers:

(1) an input layer of N nodes, each of which is an individual feature of the exemplar feature vector;

(2) a hidden layer of M nodes (M could be equal to Q for a relatively small data set, otherwise, the training data set could be reduced for efficiency by any suitable method to M exemplar vectors ($M < Q$), where each node is an exemplar vector $\vec{y}^{(m)}$ that could be an individual feature vector from the training data set or a center of a cluster within training data set; when an input feature vector $\vec{x}^{(q)}$ is put through the m-th hidden node, the Gaussian kernel of that vector $\vec{x}^{(q)}$ and vector $\vec{y}^{(m)}$ is calculated as $f_m = k(\vec{x}^{(q)}, \vec{y}^{(m)})$ and passed further in the network;

(3) an output layer of J nodes (J is the number of all possible labels (or classes) in the data set), where the inputs from all of the hidden nodes are combined in a weighted

average at each output node. The weights $\{u_{mj}\}$ are the learned gains on the lines from the hidden layer to the output layers – they get adjusted during the training phase, so that each output will match the corresponding target (targets are the numerical class labels).

The RBF NN is trained using the set of labeled feature vectors in the following fashion. Each labeled feature vector $\vec{x}^{(q)} : q = 1,...,Q$ is fed into the network and passed through all of hidden nodes where the Gaussian kernels are calculated:

$$f_m = k(\vec{x}^{(q)}, \vec{y}^{(m)}) \qquad (14)$$

where $\vec{y}^{(m)}$ is an *m*-th node exemplar feature vector and $m = 1,...,M$.

The output f_m is weighted by the corresponding weights (weights are initially set to some random numbers between 0 and 1 and updated at each iteration of the training phase) and the weighted sum is averaged over all hidden nodes at each *j*-th output node:

$$z_j = \frac{1}{M}\sum_{m=1}^{M} u_{mj} f_m \qquad (15)$$

The objective of the RBF NN algorithm is to minimize the mean square error function *E* by adjusting the weights $\{u_{mj}\}$ so that when the training phase is completed, the outputs should match the target vectors:

$$E = \sum_{j=1}^{J}(t_j - z_j)^2 = \sum_{j=1}^{J}(t_j - \frac{1}{M}\sum_{m=1}^{M} u_{mj} f_m)^2 \qquad (16)$$

Thus, to minimize *E* over all weights $u_{mj} : m = 1,...,M; j = 1,...,J$:

$$\frac{\partial E}{\partial u_{mj}} = \left(\frac{\partial E}{\partial z_j}\right)\left(\frac{\partial z_j}{\partial u_{mj}}\right) = \left(-2\sum_{j=1}^{J}\left(t_j - z_j\right)\right)\frac{f_m}{M} = 0 \qquad (17)$$

Using the steepest descent method, we can update the weights for each feature vector:

$$u_{mj}^{(k+1)} = u_{mj}^{(k)} - \frac{\partial E}{\partial u_{mj}^{(k)}}$$

$$= u_{mj}^{(k)} + \left(\frac{2\eta}{M} \sum_{j=1}^{J} \left(t_j - z_j \right) \right) f_m \qquad (18)$$

where η is a learning rate (or step size).

Upon training the RBF NN over all Q labeled feature vectors from the training data set, each new weight u_{mj} is calculated as follows:

$$u_{mj}^{(k+1)} = u_{mj}^{(k)} + \frac{2\eta}{M} \sum_{q=1}^{Q} \left(\sum_{j=1}^{J} \left(t_j^{(q)} - z_j^{(q)} \right) f_m^{(q)} \right)$$

$$= u_{mj}^{(k)} + \frac{2JQ\eta}{M} \sum_{q=1}^{Q} \left(k(\vec{x}^{(q)}, \vec{y}^{(m)}) \sum_{j=1}^{J} \left(t_j^{(q)} - z_j^{(q)} \right) \right) \qquad (19)$$

After implementing the RBF NN algorithm, it was tested by using the benchmark data set (the Wisconsin breast cancer data set). We used the reduced training set of feature vectors for the hidden nodes – we eliminated those feature vectors that were too close to others by using the fraction of the average distance between all pairs of vectors in the data set, the remaining vectors were used to form Gaussian kernels. After the network was trained, the testing data set was used to asset the quality of the RBF NN:

Table 6. The results of classification accuracy of RBF NN algorithm on the Wisconsin data set using 7-fold cross validation.

PARAMETERS: *th1; th2*	Classification Accuracy (%)	
	max	average
0.15; 0.10	66.670	55.381
0.08; 0.10	68.690	57.241
0.11; 0.10	68.690	57.813
0.10; 0.10	68.690	58.813
0.10; 0.20	60.000	53.353
0.10; 0.12	68.690	56.813
0.10; 0.09	66.670	57.667

4.2.2 Support Vector Machines (SVMs)

Kernel-based learning and data classification first appeared in the form of support vector machines (SVMs) [65], [66], [67], [68], [69], a classification algorithm that overcame many computational and statistical difficulties of previously used algorithms such as backpropagation multilayer neural networks and decision tree learning algorithms, and rapidly became the most well known and probably the most extensively used class of algorithms based on the use of kernel methods. SVMs finally made it possible to analyze nonlinear relations between data items in the high-dimensional feature space with the efficiency of linear algorithms while avoiding the problems of local minima and overfitting. Techniques based on SVMs have been used to solve problems in different areas of applied pattern analysis including classification textual

documents into a number of predefined categories [91] and handwritten character recognition [92], [93], computer vision [94], [95], bioinformatics [96], [97], and many others [98] , [99].

One of the objectives of this thesis was to compare the performance of the several different types of classifiers in order to find the best possible algorithm for this type of task. One of the characteristics that made our pattern recognition task special was the high dimensionality of the feature vectors and a quite limited set of vectors for training. If X is a set of Q exemplar feature vectors $\{\vec{x}^{(q)} : q = 1,...,Q\}$, where each vector has N features, $\vec{x}^{(q)} = (x_1^{(q)}, x_2^{(q)},..., x_N^{(q)})$, then $Q << N$ in the case of our classification problem.

Scientific research conducted in the area of pattern recognition that deals with highly dimensional vector spaces and limited numbers of exemplar vectors in the data sets, suggests that one of the best performers for this type of classification tasks is a Support Vector Machine algorithm.

Support Vector Machines (SVMs) are learning systems that "use a hypothesis space of linear functions in a high dimensional feature space, trained with a learning algorithm from optimization theory that implements a learning bias derived from statistical learning theory" [66]. The theory behind SVMs has a quite complex, but at the same time, well defined mathematical model that is built on rigorous theoretical analyses and therefore, guarantees computational efficiency. It is mostly based on statistical learning theory, notions of high dimensional vector spaces, support vectors, and kernel functions that can map vectors from one vector space to another. SVMs rely on preprocessing the data to represent patterns in a high dimensional space by mapping them

using the some transformation function $\Phi(\vec{x})$, which we don't have to know explicitly. As in the case of all kernel methods, instead of computing the mapping function $\Phi(\vec{x})$ explicitly, the SVMs algorithm replaces it with the kernel function $k(\vec{x}, \vec{s}^{(i)}) = \Phi(\vec{x}) \cdot \Phi(\vec{s}^{(i)})$, where $\vec{s}^{(i)}$ is an *i*-th support vector, and uses it for training.

Typically, the new vector space where the data become linearly separable is much higher dimensional than the original input vector space. With an appropriate nonlinear mapping to a sufficiently high dimensional vector space, data from two (or more) different categories can always be separated by a hyperplane (or several hyperplanes in the case of multiclass environment). The objective of the SVM classifier is to create a separating hyperplane with the *largest* possible margin. The larger the margin is, the better the generalization of the created classifier. The margin is normally determined by *support vectors* (Figure 20). The support vectors are the exemplar vectors from the training data set that are the closest to the hyperplane. These vectors define the optimal separating hyperplane and are the most difficult patterns to classify. In the SVM algorithm, the support vectors are the most important and informative vectors for the classification purpose. Normally, after determining support vectors, the algorithm ignores all the rest of the training set. This is one of the reasons for the computational efficiency of SVMs.

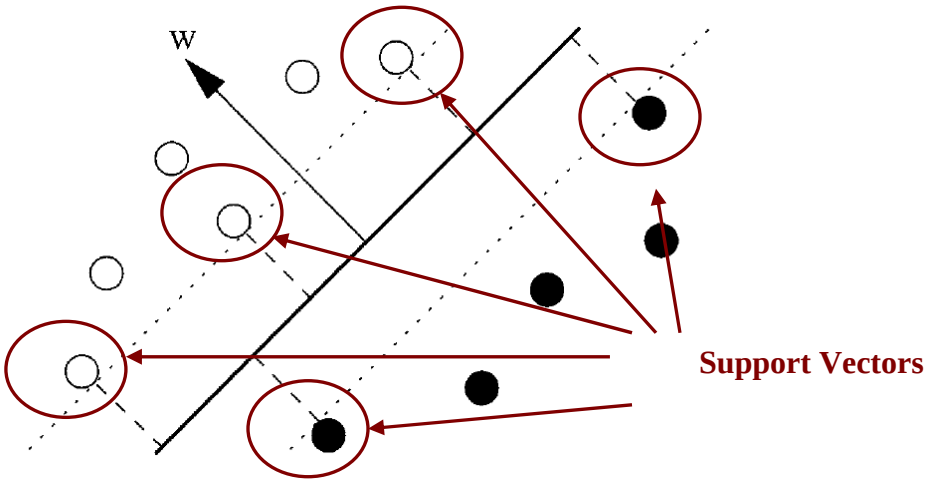

Figure 20. Separating hyperplane, margins, and support vectors: a linear classifier is defined by a hyperplane's normal vector w and margins. The margin of a linear classifier is the minimal distance of any training point to the hyperplane. On this figure it is the distance between the dotted lines and the thick line (shown by the blue bidirectional arrow). Support vectors lie on the dotted line (the margin) and are marked by the red circles around them.

In the current work we used LIBSVM – A Library for Support Vector Machines, open source implementation of linear SVM classification, specifically multiclass SVM, which is an extension of the main library for SVMs [100].

Even though SVMs were originally designed for binary classification, there exist a number of approaches to effectively extend the SVM algorithm for multiclass classification. The easiest way to do it is to combine several binary classifiers. The algorithm used for multiclass classification in the current implementation implements a *one-against-one* classification approach. Thus, if the data set consists of feature vectors from the *N* different classes, the algorithm has to construct $\frac{N \times (N-1)}{2}$ classifiers, where each one is trained on data from only two particular classes.

After all binary classifiers have been constructed the way to use them for the future testing may not be so obvious. There exist some methods for doing so, and the one that the LIBSVM implementation uses is based on a voting strategy. If during testing the algorithm has to decide for the unlabeled feature vector $\vec{x}$ between class *i* and class *j* and the discriminant function suggests that $\vec{x}$ is in *i*-th class, then the vote for class *i* is added by one, otherwise, the vote added for class *j*. After all classifiers have been tested, the class with the largest number of votes wins and $\vec{x}$ gets that class' label.

Again, we used the Wisconsin breast cancer data set as a benchmark data set to test the SVM algorithm in order to compare the results of classification with all pattern recognition algorithms developed before within the framework of the current research.

Table 7. The results of classification accuracy of SVM algorithm on the Wisconsin data set using 7-fold cross validation.

Type of kernel	Classification Accuracy (%)	
	max	average
Linear: $k^{(l)}(\vec{x},\vec{s}^{(i)}) = \vec{x}\cdot\vec{s}^{(i)}$	100.000	95.997
Polynomial: $k^{(p)}(\vec{x},\vec{s}^{(i)}) = (\vec{x}\cdot\vec{s}^{(i)})^3$	97.980	90.140
Polynomial: $k^{(p)}(\vec{x},\vec{s}^{(i)}) = (1+\vec{x}\cdot\vec{s}^{(i)})^3$	100.000	96.284
Gaussian: $k^{(g)}(\vec{x},\vec{s}^{(i)}) = \exp\left(-\frac{\| \vec{x}-\vec{s}^{(i)} \|^2}{9}\right)$	100.000	96.284
Sigmoid: $k^{(s)}(\vec{x},\vec{s}^{(i)}) = \tanh(\frac{1}{9}\times(\vec{x}\cdot\vec{s}^{(i)}))$	85.860	75.266
Sigmoid: $k^{(s)}(\vec{x},\vec{s}^{(i)}) = \tanh(\frac{1}{9}\times(\vec{x}\cdot\vec{s}^{(i)})+1)$	78.790	65.541

Traditionally, the concept of fuzzy classifiers has been built around the notion of *fuzzy set membership functions* and can be vied as, for example, a fuzzy neural network [101], [102], or a fuzzy rule-based expert system [103]. An output value of some particular fuzzy set membership function applied to an unlabeled input feature vector $\vec{x}$ is a fuzzy truth value which represents that this input feature vector belongs to some particular class with a confidence that ranges between 0 and 1. Thus, the feature vector $\vec{x}$ belongs to the class with the highest fuzzy truth value. When one of fuzzy truths for the feature vector $\vec{x}$ is significantly greater than all others, then $\vec{x}$ belongs to that particular single class, otherwise it may belong to more than once class with the given relative fuzzy truth value in each case.

Even though it is customary to view fuzzy classifiers as built upon a notion of fuzzy set membership functions, we believe that it would be more correct to consider the pattern recognition part of our classifier systems within the framework of *kernel methods* [88].

4.2.3 Fuzzy Neural Networks (FNNs)

Viewing fuzzy classifiers as fuzzy neural networks is very intuitive and therefore beneficial for clear understanding and correct utilization.

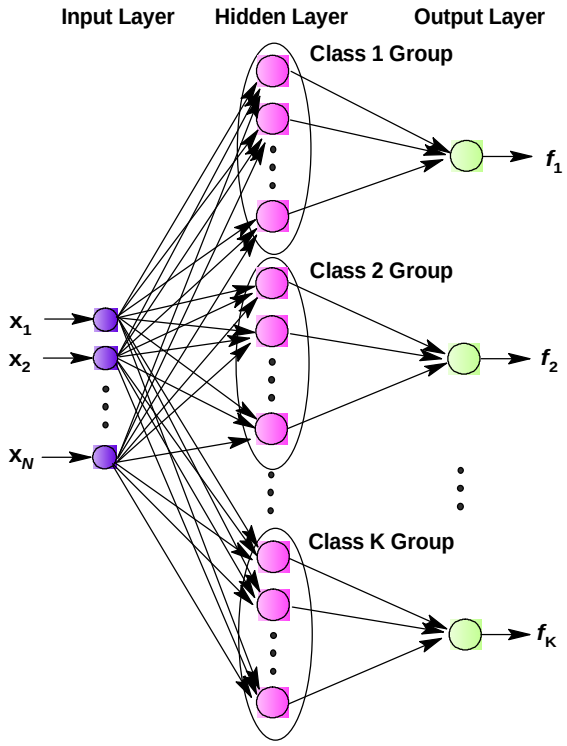

Figure 21. Representation of a fuzzy classifier as a fuzzy neural network.

In this example, there are *K* true classes in the data set; the hidden layer has been formed based on the population of labeled input feature vectors of a training data set and the information about classes. For any unlabeled feature vector $\vec{x}_i$ from the population of a test data set of feature vectors $\vec{x}_1$ through $\vec{x}_Q$, the fuzzy set membership functions $f_j(x_i)$ can be calculated in the term of fuzzy set membership functions, for example, as following:

$$f_1(x_i) = \frac{1}{Q_1}\sum_{q_1=1}^{Q_1}\exp\left(-\frac{\| \vec{x}_i - x^{(q_1)} \|^2}{2\sigma_1^2}\right) \qquad (20)$$

$$f_2(x_i) = \frac{1}{Q_2}\sum_{q_w=1}^{Q_2}\exp\left(-\frac{\| \vec{x}_i - x^{(q_2)} \|^2}{2\sigma_2^2}\right)$$

: :

$$f_K(x_i) = \frac{1}{Q_K} \sum_{q_K=1}^{Q_2} \exp\left(- \frac{\| \vec{x}_i - x^{(q_K)} \|^2}{2\sigma_K^2} \right)$$

where Q_1, Q_2,…, Q_K are the number of feature vectors in class 1, class 2, … class K respectively; $\vec{x}^{(q_j)}$ is q-th feature vector of class j.

Fuzzy Neural Networks (FNNs) are the simplest class of fuzzy classifier systems: their nodes do not have weights and they do not require extensive training. Since we constructed our FNN within framework of the kernel methods, we consider our classifier to be based on "kernelization" of the metric for measuring distances between the centers of clusters that were established in the input space and the unlabeled feature vectors, as was shown before (Eq. 9):

$$\| \Phi(\vec{x}) - \Phi(\vec{x}^{(q_j)}) \|^2 = k(\vec{x}, \vec{x}) + k(\vec{x}^{(q_j)}, \vec{x}^{(q_j)}) - 2k(\vec{x}, \vec{x}^{(q_j)}) \qquad (21)$$

where $\vec{x}$ is an arbitrary unlabeled feature vector from the test data set and $\vec{x}^{(q_j)}$ is a q-th feature vector of class j in the training data set. Since $k(\vec{x}, \vec{x})$ and $k(\vec{x}^{(q_j)}, \vec{x}^{(q_j)})$ are both constants (and equal to 1) then, in order to find the closest labeled feature vector to the given unlabeled feature vector, we should look for the greatest value of the kernel – in our case the Gaussian kernel (Eq. 12):

$$k^{(g)}(\vec{x}, \vec{x}^{(q_j)}) = \exp\left(- \frac{\| \vec{x} - \vec{x}^{(q_j)} \|^2}{2\sigma_j^2} \right) \qquad (22)$$

where σ_j is a variance of the j-th class in the training data set. If the data of the given class has been proven not to contain outliers (feature vectors that are numerically distant from the rest of the data) or mislabeled feature vectors, the variance can be

computed as a fraction (between $\frac{1}{3}$ and $\frac{1}{2}$) of the average distance between every two labeled feature vector within class *j*.

We tried two different approaches in constructing our fuzzy classifier.

In the first approach, we construct a discriminant function as the maximum kernel value for the unlabeled feature vector $\vec{x}$ and every labeled feature vector within each class:

$$f_j^1(\vec{x}) = \{\max\{k(\vec{x}, \vec{x}^{(q_j)}) : q_j = 1,...,Q_j\} \quad (23)$$

where $f_j^1(\vec{x})$ is the first constructed discriminant function for unlabeled feature vector $\vec{x}$ over class *j*; $k(\vec{x}, \vec{x}^{(q_j)})$ is a Gaussian kernel as in (Eq. 12); $\vec{x}^{(q_j)}$ is a *q*-th feature vector of class *j* in the training data set, $q_j = 1,...,Q_j$; and Q_j is the total number of feature vector in class *j*.

In the second approach, instead of using the maximum kernel values for an individual feature vector over each class, the algorithm uses the average value of all possible kernel values in each class:

$$f_j^2(\vec{x}) = \frac{1}{Q_j}\sum_{q_j=1}^{Q_j} k(\vec{x}, \vec{x}^{(q_j)}) \quad (24)$$

where $f_j^2(\vec{x})$ is the second constructed discriminant function for unlabeled feature vector $\vec{x}$ over class *j* and everything else is as above.

After evaluating the discriminant functions for all classes, the labeling procedure is straightforward: the unlabeled vector $\vec{x}$ from the test set belongs to the class for which the discriminant function has the largest value.

After testing this algorithm and using both discriminant functions, we found that the classifier that uses the second discriminant function provides noticeably higher classification accuracy:

Table 8. The results of classification accuracy of FNN algorithm on the Wisconsin data set using 7-fold cross validation.

Threshold value for computing σ	$f^1(\vec{x})$		$f^2(\vec{x})$	
	max	average	max	average
0.09	97.000	88.179	98.000	92.709
0.10	97.000	88.179	98.000	93.139
0.11	97.000	88.179	98.000	93.281
0.15	97.000	88.274	98.000	94.854
0.20	97.000	88.274	100.000	96.140
0.25	97.000	88.274	100.000	96.283
0.30	97.000	88.274	100.000	96.286

4.2.4 Clustering-Based Fuzzy Classifiers

It is worth noting that the term clustering is often used with different meanings in different fields of science. In computer science, clustering refers to a technique or tool that attempts to discover an internal structure or certain patterns in a given data set without making any *a priori* assumptions. Thus, clustering is the unsupervised classification of unlabeled feature vectors with the objective of finding a convenient and valid organization of the data into classes or categories. By clustering the data we partition the given data set into groups or *clusters* in such a way that any two pieces of

data from the same cluster are as similar as possible and any two pieces of data from different clusters as dissimilar as possible.

Although traditionally clustering deals with unlabeled data, which are data items that contain no class information attached to them, and is considered a method of unsupervised learning, clustering is very useful in implementing a "divide and conquer" strategy to reduce the computational complexity of various decision-making algorithms in pattern recognition. For example, initial clustering of the data is widely used in popular techniques in pattern recognition such as the nearest-neighbor decision rule [104] or for problem localization [105].

In our case, class information for a training set of feature vectors is available. It might seem that the use of unsupervised learning methods, such as clustering, is not necessary. However, we have found that having established the internal structure in our data set first through clustering the data helps us tremendously in finding the rules for assigning the unlabeled data items to correct classes. Data could be noisy, contain outliers or missing features, or could be labeled incorrectly. Cluster analysis, as the most prominent example of unsupervised learning, is very good at dealing with all these and many other similar cases.

The experimental data we collected during our experiments with chemical vapors were sometimes slightly, sometimes noticeably different from day to day. This effect happened even though all formal experimental conditions (such as the concentration of chemical vapors in the gaseous mixture, the temperature of the array cell, etc.) were the same. This was mostly due to the fact that some parameters of our experimental setup and some experimental conditions could not be reproduced precisely or controlled completely

each time. One such parameter is the low precision of the settings of the device that creates the desirable concentration of chemical vapors in the gaseous mixture. The imprecision in that device's settings resulted in sometimes considerably different real concentrations of chemical vapors created from one experiment to another. Thus, it would be quite difficult to "explain" to our algorithm how sometimes quite different feature vectors (that were created from the data collected on different days) can belong to the same class. We thought that unsupervised learning such as fuzzy clustering in our case might actually help us with this problem. The algorithm would naturally partition training vectors from the same class into several different clusters (if the necessity arises) and increase the chances of correct classification of the unseen exemplar vectors.

For both our fuzzy clustering algorithms, we performed a pre-clustering procedure, whose goal is reducing the data set for efficiency. Pre-clusters are the result of preliminary partitioning of the data set and they can be considered as some sort of proto-clusters. Pre-clusters are typically very compact and have a hyperspherical shape. We used an improved *k*-means clustering algorithm for this purpose.

4.2.4.1 Pre-clustering by Improved *K*-Means Clustering

The *k*-means algorithm is one of the most popular clustering methods – it is very simple, straightforward, and robust; therefore, it has been used in a wide spectrum of applications [106]. This algorithm employs the most intuitive and frequently used criterion function in partitional clustering – the squared error criterion:

$$F(\{C^{(1)},\ldots,C^{(K)}\}) = \sum_{j=1}^{K}\sum_{i=1}^{Q_j} \| \vec{x}^{(i_j)} - \vec{c}^{(j)} \|^2 \qquad (25)$$

where K is the number of clusters in the data set; $C^{(1)},...,C^{(K)}$ are K clusters that the data set has been partitioned into; Q_j is the number of feature vectors in each cluster; $\vec{x}^{(i_j)}$ is the i^{th} feature vector belonging to the j^{th} cluster, $C^{(j)}$; and $\vec{c}^{(j)}$ is the center of the cluster $C^{(j)}$.

The *k*-means algorithm works as following:

(1) Select the initial K cluster centers randomly over the input domain.

(2) Assign each feature vector to its closest cluster center and compute the new cluster centers as cluster prototypes. Repeat this step until convergence is achieved, e.g., there is no reassignment of any feature vector from one cluster to another, or the criterion function doesn't change noticeably anymore.

(3) Merge and split clusters based on some heuristic information, optionally repeating step (2).

As can be deducted from the above algorithm description, the traditional *k*-means algorithm requires *a priori* knowledge about the number K of clusters in the data set, which often is unknown beforehand, and can suffer from bad or unfortunate initial cluster centers selection [107]. We looked for improvements of the *k*-means algorithm similar to those described in [108] and [109] that would significantly reduce the algorithm's drawbacks. Since we didn't have to deal with guessing the number of possible classes in the data set or handling problems that large data sets normally bring with them, our task became significantly easier than the typical case of partitioning of unknown data set within framework of unsupervised learning.

After a number of experimentations, we developed two modifications of the improved *k*-means algorithm. The first modification was for establishing the initial pre-clusters in the Fuzzy *C*-Means (FCM) clustering algorithm:

Calculate the test threshold as a fraction of an average distance between all possible pairs of feature vectors in the initial data set.

Instead of starting with *K* random initial points as cluster centers or an empty set of centers, start with the maximally possible number of centers, *Q*, where *Q* is the number of all feature vectors in the set. Next, eliminate the feature vectors that are too close to other centers from the set of possible cluster centers using the threshold value and assign the eliminated feature vector to the closest center.

On each iteration, the feature vectors that were eliminated from the set of centers are checked once again against the new center that is under examination: if the distance from some vector that was assigned to another center before to current center is less than the distance to its previous center, reassign this point to the current center. This newly added modification to the clustering procedure is very important as it eliminates the dependency of the clustering procedure on the order of instantiating the initial cluster centers and merging feature vectors in the pre-clusters.

After the tentative number of initial cluster centers has been established, the algorithm calculates the number of vectors in each cluster. The clusters that contain a smaller number of vectors than was specified by a programmer or user are eliminated as well. The vectors from those clusters are assigned to the nearest neighboring clusters. From this point, the algorithm continues clustering using an improved *k*-means clustering algorithm: at each iteration, it keeps recalculating the cluster centers, reassigning all

vectors to the newly created cluster centers, and eliminating those clusters that contain fewer vectors than a given threshold. The algorithm repeats this processing until the set of the cluster centers remains unchanged.

For our second fuzzy clustering algorithm, fuzzy connectivity clustering, we made further modification into the improved *k*-means algorithm, since we had more flexibility in preprocessing the training data.

First, we wanted to automate the adjustment of the number of pre-clusters and make it independent from the user pre-settings. For this purpose, we chose the permitted range for the number of initial pre-clusters in the data set first. The number of preliminary clusters (or pre-clusters) should correlate with the number of true classes, which is known in our case. We normally use the range: $2 \times N \le K \le 15 \times N$, where N is the number of true classes and K is the final number of pre-clusters.

Initially, the algorithm calculates the test threshold as a fraction of an average distance between all possible pairs of feature vectors in the data set. After that, it automatically adjusts the threshold value for eliminating centers based on their proximity to other centers so that the final number of pre-clusters fits into the given range; that is, if the number of pre-clusters are greater than the maximum number in the specified range, the program increases the threshold value by the specified learning rate, if the number of pre-clusters are less than the minimum number in the specified range, it decreases the threshold value by the specified learning rate.

Second, we now allow having single-point clusters, which are typically outliers. Thus, we do not enforce any rule in this modification of the improved *k*-means algorithm

such as that each cluster has to have at least a few feature vectors as we did before (normally, this number is five or more).

Using this particular modification of the improved *k*-means algorithm we do not have to worry about the outliers; therefore, we do not have to calculate the trimmed mean of each pre-cluster, since the embedded requirement to the pre-clusters to be compact excludes the possibility of outliers to be included in any of them.

After the desirable number of pre-clusters has been established, the program calculates the means of all pre-clusters and uses those means as a final set of cluster centers. Typically, each resulting cluster contains several pre-clusters. This permits resulting clusters to take their own natural shape, which is not necessarily hyperspherical.

4.2.4.2 Fuzzy Clustering

Since fuzzy models for pattern recognition became popular among scientists, engineers, and statisticians in trying to reflect vagueness and imprecision of boundaries between group of objects in real applications, numerous *fuzzy clustering* algorithms, whose aim is to model fuzzy, i.e., ambiguous and vague, unsupervised patterns efficiently have emerged [62], [63], [64]. In classical or crisp clustering analysis, any piece of data, i.e., feature vector, can be assigned to only one cluster. Fuzzy clustering has removed that constraint – it allows each feature vector in the data set to belong to more than one cluster with different membership degrees (between 0 and 1) and vague or fuzzy boundaries between clusters. Thus, fuzzy clustering offers an opportunity to deal with real-life data that belong to more than one group, or class, at the same time; as for the feature vector

membership degree – it provides a measure of degree to which the given feature vector fits within a particular class.

Both our fuzzy clustering algorithms take the following input files:

- *data files* – there are two files, one contains the training data set, the other contains the testing data set; each file contains the dimension of the feature vectors, the number of vectors in the current data set and vectors themselves (as a table of row vectors). The last field of each vector is a numerical representation of the class that the given vector belongs to;
- *description file* – the file contains the full description of all classes presented in the training set, including the numerical class label used in the data sets.

In the training phase, the program reads in the training and testing data sets and the description of the classes used for training. We assume that the testing data set contains samples from the same pool of classes, i.e. there are no feature vectors in the testing set that belong to the classes that are not present in the training data set

In the next step, the program preprocesses training set into pre-clusters using the improved *k*-means algorithm described above. After the set of pre-clusters has been established by mean of the improved *k*-means algorithm, our algorithm continues clustering using the standard FCM algorithm with some minor modifications or the fuzzy connectivity clustering algorithm (FCC).

4.2.4.3 Fuzzy Classifier based on Fuzzy *C*-Means Clustering (FCM-based)

Bezdek developed a family of clustering algorithms, based on a fuzzy extension of the least-squared error criterion [62], [110]. The FCM algorithm is one of them – it is a

set-partitioning method based on Picard iteration through necessary conditions for optimizing a weighted sum of squared errors objective function J_m (Eq. 26) [111].

If $X = \{\vec{x}_1, \vec{x}_2, ..., \vec{x}_Q\}$ is a finite set of feature vectors in *N*-dimensional Euclidean space $\Re^N$, then the goal of the FCM algorithm is to partition this set into *C* clusters represented as fuzzy sets $F^{(1)}, F^{(2)}, ..., F^{(C)}$ by minimizing the objective function $J_m(U, V)$ with respect to *U*, a fuzzy *C*-partition of the data set, and to *V*, a set of *C* cluster prototypes (a *cluster prototype* is a vector that represents its cluster; in our case it is just a center of a given cluster):

$$J_m(U,V) = \sum_{k=1}^{Q} \sum_{i=1}^{C} u_{ik}^m d^2(\vec{x}^{(k)}, \vec{v}^{(i)}) \qquad (26)$$

In (Eq. 26) *m* is any real number greater than 1 (this is weighting exponent for u_{ik}, or fuzzifier), the value that controls the "fuzziness", in other words, how much clusters may overlap. This parameter reduces the sensitivity of the cluster centers to noise in the data). Variable $\vec{x}^{(k)}$ is the *k*-th *N*-dimensional feature vector, $\vec{v}^{(i)}$ is the prototype (a center) of the *i*-th cluster, u_{ik} is the degree of membership of x_k in the *i*-th cluster, $d^2(\vec{x}^{(k)}, \vec{v}^{(i)})$ is an inner product metric (distance between vector x_k and cluster center v_i), *Q* is the number of feature vectors, and *C* is the resulting number of clusters.

The computation of the degree of membership u_{ik} depends on the definition of the distance measure, $d^2(\vec{x}^{(k)}, \vec{v}^{(i)})$:

$$d^2(\vec{x}^{(k)}, \vec{v}^{(i)}) = (\vec{x}^{(k)} - \vec{v}^{(i)})^T \Sigma^{-1} (\vec{x}^{(k)} - \vec{v}^{(i)}) \qquad (27)$$

where Σ is an arbitrary covariance matrix.

In the current work we assume that the shape of all clusters is hyperspherical, so the covariance matrix in our case is equal to the identity matrix *I*. Thus, the distance $d^2(\vec{x}^{(k)}, \vec{v}^{(i)})$ in our case is Euclidean, as was described in the beginning of the current chapter (Eq. 1):

$$d^2(\vec{x}^{(k)}, \vec{v}^{(i)}) = \sum_{i=0}^{N} \left(x_i^{(k)} - v_i^{(i)}\right)^2 = \| \vec{x}^{(k)} - \vec{v}^{(i)} \|^2 \qquad (28)$$

where *N* is the dimension of the feature vectors.

Typically, the FCM algorithm starts by choosing the number of clusters *C* and the value of fuzzifier *m* (both parameters are chosen by a user), and by randomly initializing the membership degree matrix *U* under the constraint such that $\sum_{i=1}^{C} u_{ik} = 1$ (the sum of memberships for each feature vector over all clusters should be equal to 1). Next, the initial cluster prototypes are computed, using the following formula:

$$\vec{v}^{(i)} = \frac{\sum_{k=1}^{N} (u_{ik})^m x_k}{\sum_{k=1}^{N} (u_{ik})^m} \qquad (29)$$

Following this step, using the computed cluster prototypes, the fuzzy memberships u_{ik} are updated according to the equation:

$$u_{ik} = \frac{\left(\frac{1}{d^2(\vec{x}^{(k)}, \vec{v}^{(i)})}\right)^{\frac{1}{m-1}}}{\sum_{i=1}^{c} \left(\frac{1}{d^2(\vec{x}^{(k)}, \vec{v}^{(i)})}\right)^{\frac{1}{m-1}}} \qquad (30)$$

Next, the algorithm iterates between (Eq. 29) and (Eq. 30) until the memberships or cluster centers for successive iteration differ by less than some termination criterion, ε, chosen by a programmer or user.

It is quite obvious that the standard FCM algorithm, similarly to the standard *k*-means algorithm described before, is very sensitive to the initial choice of cluster centers. Different choices of cluster prototypes may lead to convergence to different local optima, in other words, to different partitions. In many practical situations *a priori* knowledge of the approximate locations of the initial centers does not exist, and in order to achieve optimal partition unsupervised tracking of classification prototypes is required.

That is why making a preliminary assessment of the data set structure provides invaluable advantages over the standard approach. Thus, we used the pre-cluster centers obtained by running the improved *k*-means algorithm as a starting point for the modified FCM algorithm. Therefore, we did not have to guess the fuzzy memberships u_{ik}: we started the main loop of the FCM algorithm by *calculating* those memberships (Eq. 30).

After the algorithm converges, class labels have to be assigned to each feature vector. The quality of clustering is indicated by how closely the feature vectors are associated to the cluster centers, and the level of association or classification is measured by the membership functions. If the value of one of the memberships is significantly larger than the others' for a particular data point, then that data point is identified as being a part of the subset of the data represented by the corresponding cluster center. Thus, larger membership values indicate higher confidence in the assignment of the feature vector to the particular cluster.

We said before that the goal of the FCM algorithm is to partition some arbitrary set $X = \{x_1, x_2, \ldots, x_Q\}$ into C clusters (subgroups) represented as fuzzy sets $F^{(1)}, F^{(2)}, \ldots, F^{(C)}$. Generally speaking, in fuzzy clustering each cluster (each fuzzy set $F^{(i)}$, $1 \le i \le C$) is a fuzzy set of *all* feature vectors, that is each $F^{(i)}$ includes *all* data points but with different values of fuzzy membership.

In the current research, our goal was to assign class labels to each data point as one does in hard clustering, meaning that at the end, each data point should belong to one and only one class (but probably, with different level of confidence). Thus, in our study, fuzzy clustering was only an auxiliary tool for reaching the ultimate goal – to discover structures or certain groupings in a data set and therefore a set of rules that significantly facilitate the process of correct labeling of newly encountered, unseen before unlabeled feature vectors.

Consequently, after the FCM algorithm converges (in our case, when either memberships or cluster centers for successive iteration differ by less than the termination criterion $\varepsilon = 0.00001$), the algorithm performs "hard" partitioning, meaning that at the end each feature vector would belong to one and only one cluster, that is, to the cluster whose membership function for this vector is the largest. At this point, the algorithm labels the finally created clusters according to the "description file" and calculates some statistics. It might happen that some clusters contain vectors from the different classes. If that is the case, the algorithm calculates its confidence in class labeling according to the percentage of the vectors from the major class in that cluster.

At this point the algorithm enters a pattern recognition phase. After the labeled feature vectors have been clustered and each cluster was labeled as described above, we

constructed the fuzzy classifier over it. Again, we consider the fuzzy classifier within framework of kernel methods, but this time it was built around clusters that the training data set was partitioned into. And as in the case of FNN, we tried two different approaches for designing a fuzzy classifier.

In the first approach, for each unlabeled feature vector $\vec{x}$ the algorithm calculates the value of a Gaussian kernel of this feature vector and each center of all clusters. In order to assign a given feature vector to one of those clusters, we have to evaluate a discriminant function $f_j(\vec{x})$, which is in this case just a Gaussian kernel with σ_j being the variance of the *j*-th cluster, for all *C* final clusters ($j = 1,...,C$):

$$f_j^1(\vec{x}) = k(\vec{x}, \vec{v}^{(j)}) \qquad (31)$$

where $f_j^1(\vec{x})$ is a discriminant function of type 1 for unlabeled feature vector $\vec{x}$ over cluster *j*; $\vec{v}^{(j)}$ is a center of the *j*-th cluster; $k(\vec{x}, \vec{v}^{(j)})$ is a Gaussian kernel. The cluster that has the largest discriminant function value is considered to be the winner, and the unlabeled feature vector is get assigned to this cluster.

In the second approach, instead of using only the centers of the clusters, the discriminant function is constructed to be equal to the maximum kernel value in each cluster:

$$f_j^2(\vec{x}) = \max\{k(\vec{x}, \vec{x}^{(q_j)}) : q_j = 1,...,Q_j\} \qquad (32)$$

where $f_j^2(\vec{x})$ is a discriminant function of type 2 for unlabeled feature vector $\vec{x}$ over cluster *j*; $x^{(q_j)}$ is a feature vectors that belongs to the *j*-th cluster, *j* = 1,…,*C*, $q_j = 1,...,Q_j$; Q_j is the total number of feature vector in the *j*-th cluster; and $k(\vec{x}, \vec{x}^{(q_j)})$ is

a Gaussian kernel, calculated for the unlabeled feature vector $\vec{x}$ and the *q*-th feature vector of the *j*-th luster. As in the previous case, the unlabeled feature vector $\vec{x}$ gets assigned to the cluster that has the largest value of the discriminant function $f_j^2(\vec{x})$.

After the unlabeled feature vector has been assigned to some cluster, it also gets a label from the cluster. If the "winning" cluster has high confidence in its label, i.e. the absolute majority of the vectors in that cluster belong to the same class, we have high confidence in the performed classification. Otherwise, our confidence might be as low as the percentage of the major class in the given cluster (e.g., 80%, or even 70%, but this is rarely the case).

After testing the current algorithm by using the benchmark data set (the Wisconsin breast cancer data set), we found that the classifier based on the discriminant function of type 2 gives higher accuracy of classification.

Table 9. The results of classification accuracy of FCM-based algorithm on the Wisconsin data set using 7-fold cross validation.

PARAMETERS*: q; th1; th2; f	$f^1(\vec{x})$		$f^2(\vec{x})$	
	max	average	max	average
20; 0.10; 0.25; 1.2	97.980	80.140	97.000	91.137
15; 0.10; 0.25; 1.2	94.000	80.560	99.000	92.713
12; 0.10; 0.25; 1.2	92.000	82.839	100.000	90.706
10; 0.10; 0.25; 1.2	92.000	84.697	100.000	92.710
8; 0.10; 0.25; 1.2	96.970	86.996	100.000	94.143
8; 0.11; 0.25; 1.2	96.970	85.424	100.000	95.429
8; 0.12; 0.25; 1.2	93.000	88.974	100.000	93.989
8; 0.08; 0.25; 1.2	96.000	81.419	100.000	90.569
8; 0.11; 0.20; 1.2	96.970	85.424	100.000	95.429
8; 0.11; 0.10; 1.2	96.970	85.424	100.000	95.429
8; 0.11; 0.40; 1.2	96.970	85.424	100.000	95.429
8; 0.11; 0.25; 1.1	96.000	89.416	98.000	93.569
8; 0.11; 0.25; 1.3	93.000	78.264	98.900	90.557

* *q* – the minimum number of vectors in each cluster; *th1* – the threshold value for the minimum distance between two cluster centers in order to keep both of these centers for further clustering; *th2* – the threshold value for cluster's variance; *f* – weighting component for fuzzy membership function (fuzzifier).

4.2.4.4 Fuzzy Classifier Based on Fuzzy Connectivity Clustering (FCC-based)

The notion of "degree of connectedness" was first introduced in the context of studying the topology and geometry of fuzzy subsets [112], [113]. In 1996, almost twenty years later after its first introduction, the concept of *fuzzy connectedness*, or *fuzzy*

connectivity, was fully explained and successfully applied for image segmentation [114]. This seminal work replaced the notion of "hanging-togetherness" for image elements with the concept of fuzzy connectedness between them: the closer two points are and the greater the similarity between them, the higher the degree of fuzzy connectivity is. This presented a solid theoretical framework and reliable computational tools for the theory of fuzzy connectedness, including the use Gaussian functions among other functions as a measurement of fuzzy connectivity between two image elements.

The fuzzy connectedness methods have been extensively and successfully used mostly in medical imaged analysis, including Multiple Sclerosis lesion quantification [115], [116], brain tumor assessment [117], breast density quantification via mammograms [118], CT colonography [119], [120], but also in some other areas of image analysis and processing, such as document analysis [121], processing of color images [122], and handwritten character recognition [123]. This concept of fuzzy connectedness was successfully extended from image elements to any other arbitrary objects to be exploited in clustering analysis [124].

In this thesis we examined this concept and extended the framework of fuzzy connectedness, or connectivity, to create a solution to our specific pattern recognition problem.

From the standpoint of kernel methods, the fuzzy connectivity clustering algorithm is a pure essence of the kernel methods. Not only is its final discriminant, or *pattern*, function built on a kernel function, but also the initial data have been processed using a kernel to create a *kernel matrix* (also known as a *Gram matrix*), which in turn is processed by a pattern analysis algorithm to produce the final discriminant function. The

discriminant function is used to process the unlabeled feature vectors with the intent of correctly recognizing them. Therefore, all stages of this particular algorithm are involved in the application of kernel methods.

Since the intermediate step of our algorithm is to create a kernel matrix, memory constraints may make it impossible or inefficient to store the full kernel matrix in memory for relatively large data sets. If this is the case, we might want to include an automatic step for reducing the initial data set for efficiency into our algorithm. Again, we have found it very efficient to use the improved *k*-means clustering algorithm described above for the purpose of data reduction. While using the version of improved *k*-means clustering that allows us to have single-point clusters, we protect ourselves from outliers and mislabeled exemplar feature vectors affecting our classification accuracy. Moreover, by keeping the pre-clusters small, compact, and perfectly hyperspherical, we avoid guessing the possible shape of the final clusters, which could be completely arbitrary.

After creating a set of L feature vectors $S = \{\vec{x}^{(1)},...,\vec{x}^{(L)}\}$, where each vector $\vec{x}^{(i)} \in S$ could be either a center of one of the pre-clusters (where $2 \times N \le L \le 15 \times N$, with N is the number of true classes in the data set) or a feature vector from the training data set itself (in the case of small data sets or if the given vector is an outlier), the FCC algorithm creates an $L \times L$ kernel matrix K whose entries are the inner products of the images of the vectors in a feature space F with a feature map Φ:

$$\mathrm{K}_{ij} = (\Phi(\vec{x}^{(i)}) \cdot \Phi(\vec{x}^{(j)})) =< \Phi(\vec{x}^{(i)}), \Phi(\vec{x}^{(j)}) >= k(\vec{x}^{(i)}, \vec{x}^{(j)}) \qquad (33)$$

$$\begin{matrix} k(\vec{x}^{(1)},\vec{x}^{(1)}) & k(\vec{x}^{(1)},\vec{x}^{(2)}) & \cdots & k(\vec{x}^{(1)},\vec{x}^{(L)}) \\ k(\vec{x}^{(2)},\vec{x}^{(1)}) & k(\vec{x}^{(2)},\vec{x}^{(2)}) & \cdots & k(\vec{x}^{(2)},\vec{x}^{(L)}) \\ \vdots & \vdots & \ddots & \vdots \\ k(\vec{x}^{(L)},\vec{x}^{(1)}) & k(\vec{x}^{(L)},\vec{x}^{(2)}) & \cdots & k(\vec{x}^{(L)},\vec{x}^{(L)}) \end{matrix} \qquad (34)$$

By the intrinsic properties of the kernel functions, the matrix K is symmetric since $K_{ij} = k(\vec{x}^{(i)},\vec{x}^{(j)}) = k(\vec{x}^{(j)},\vec{x}^{(i)}) = K_{ji}$, that is $K^T = K$. Furthermore, since we are using the Gaussian kernel, all diagonal elements of K are all 1's and therefore, all we need to store in memory is the strictly upper triangular part of the kernel matrix K, thus saving the memory resources significantly:

$$\begin{matrix} k(\vec{x}^{(1)},\vec{x}^{(2)}) & k(\vec{x}^{(1)},\vec{x}^{(3)}) & \cdots & k(\vec{x}^{(1)},\vec{x}^{(L)}) \\ & k(\vec{x}^{(2)},\vec{x}^{(3)}) & \cdots & k(\vec{x}^{(2)},\vec{x}^{(L)}) \\ & & \ddots & \vdots \\ & & & k(\vec{x}^{(L-1)},\vec{x}^{(L)}) \end{matrix} \qquad (35)$$

All the information the pattern analysis algorithms can gather about the training data and chosen feature space is contained in the kernel matrix together with any labeling information [88]. Once the kernel matrix has been established, it not only provides us with a way to estimate the number of resulting clusters within the data set, but it also allows the resulting clusters to have their natural forms and shapes that are often far from being perfectly hyperspherical.

The algorithm we created for this thesis automatically groups the pre-clusters together based on the degree of closeness (similarity, affinity, or connectedness). It is often the case that the resulting clusters contains several hyperspherical pre-clusters; sometimes the feature vectors bearing the same class label form separate resulting clusters (or groups), which is quite understandable considering for example the fact that

some important attribute (or features) that cause the vectors with the same class label be in some way different are subtle or failed to be captured by the feature extraction procedure. Sometimes the outliers could be the reason for that. The outliers can be a part of the data as a result of some type of errors in measurements or malfunctioning of reading device.

One of the major advantages of the current algorithms is that it enables us to identify the outliers and mislabeled samples during the training phase and either eliminate them from the data set completely or significantly decrease their influence on the results of classification accuracy during the pattern recognition phase.

After the algorithm groups the pre-clusters together in the resulting clusters, it labels each cluster (going largely to what had been previously described for other clustering algorithms). The advantage of this algorithm is that since we don't force the resulting clusters to be hyperspherical but rather let them have their natural shape, the confidence in the class label is significantly higher for this particular algorithm than in the case of clustering by the improved *k*-means and fuzzy *c*-means algorithms described above.

To process unseen before feature vectors with the intent of labeling them, the algorithm uses the discriminant function:

$$f_j(\vec{x}) = k(\vec{x}, \vec{v}^{(j)}) \qquad (36)$$

where $f_j(\vec{x})$ is a discriminant function applied to an unlabeled feature vector $\vec{x}$ over cluster *j*; $\vec{v}^{(j)}$ is a center of the *j*-th cluster (or just a feature vector from the training data set in case of outliers or small training data sets); $k(\vec{x}, \vec{v}^{(j)})$ is a Gaussian kernel, and

the parameter σ used in that kernel function is either a variance of cluster j or some fraction of the average distances between all pairs in the reduced data set. The cluster that produces the largest value of the discriminant function is considered to be a winner. Then, the unlabeled feature vector gets the same class label as the winning cluster has. The confidence in the assigned class labeled is solidly based on the percentage of feature vectors with the same label over all feature vectors that found to be fuzzy connected through the kernel matrix and were grouped into the same cluster.

We implemented the fuzzy connectivity clustering (FCC) algorithm in C++ using the object-oriented approach (see Appendix B for implementation details). The OOP of FCC algorithm implementation is highly beneficial compared to the procedural approach that was used in our other implementations: it reduces the program's complexity significantly, makes the program interface more informative and considerably increases the overall program's clarity, and more importantly, it facilitates the maintainability of the program and substantially simplifies further modifications, changes, and extensions of the program.

Next, the FCC algorithm was tested by using the Wisconsin breast cancer data set as a benchmark data set. While tuning the parameters of the FCC algorithm to reach out the highest possible classification accuracy, we found that the range of the number of possible pre-clusters created during the execution of the algorithm is one of the parameters that the current algorithm is very sensitive to.

It has been shown that the best classification results were obtained when we set the number of possible pre-clusters between times 2 and times 4 of the number of available classes in the set. The following table shows the results for different number of

pre-clusters selected beforehand; the values for all other parameters have been optimized in previous testing runs.

Table 10. The results of classification accuracy of FCC-based algorithm on the Wisconsin data set using 7-fold cross validation.

Number of Pre-clusters L (based on the number of true classes N in the data set)	Classification Accuracy (%)	
	max	average
$N \times 2 \le L \le 7$	99.000	94.711
$N \times 2 \le L \le 6$	99.000	95.284
$N \times 2 \le L \le 5$	100.000	95.999
$N \times 2 \le L \le 4$	100.000	96.283
$N \times 2 \le L \le 3.5$	100.000	96.427
$N \times 2 \le L \le 3$	100.000	96.713
$N \times 2 \le L \le 2.5$	100.000	96.713
$N \times 2 \le L \le 2$	100.000	96.427

By relaxing constraints on the number of possible initial pre-cluster in the training data set, we found that it is very important to keep the ratio of two parameters: a threshold value for the average distance between pre-cluster centers for calculating variances and a threshold for interpreting the fuzzy connectivity matrix less than or equal to 1. If this ratio is 1.5 or greater than the classification accuracy may drop from 99%(max)/96.141%(average) to as low as 99%(max)/85.118%(average).

Another interesting modification of the current algorithm that we created was the semi-supervised version of fuzzy connectivity clustering. Instead of separating the training and testing sets and performing the learning phase of the algorithm using just the

training set, we combined both sets (leaving feature vectors from the testing set unlabeled) and performed initial pre-clustering followed by the linking procedure through the kernel matrix over the entire data set. This idea makes a lot of sense because it simplifies the algorithm quite significantly while keeping classification accuracy almost as high as in the original longer version. The results for classification accuracy for this version varied between 100%(max)/96.284% (average) under the constraints that the number of pre-clusters should be at most 3.5 times greater than the number of true classes in the set and 100%(max)/96.426% (average) without such a constraint.

Interestingly, by eliminating a few feature vectors from the data set (less than 4%) that have been consistently misclassified or linked with feature vectors from the "wrong" class, we easily reached almost 100% in the classification accuracy on average (for both modifications of the algorithm).

5 Experimental Results

For the current thesis, we collected experimental results using the same microfabricated cantilever sensor array. This sensor array had been extensively exploited for the experimental testing for nearly three months, which significantly exceeded the most optimistic estimate of its life expectancy.

After removing especially noisy and inconsistent data, we obtained 85 34-dimensional feature vectors from nine different classes:

Table 11. Class labels according to the presence of the specified concentration of different chemical vapors in the analyzed gaseous mixture and the number of feature vectors in each class.

Analyte	26%		18%		7%	
	Class Number	Number of Vectors	Class Number	Number of Vectors	Class Number	Number of Vectors
Acetone	1	11	2	29	3	6
Ethanol	4	7	5	6	6	7
Toluene	7	11	8	3	9	8

Although we kept the experimental conditions identical throughout all experiments, the collected data were not of equal quality. The data gathered during the last month of the testing experiments revealed that the sensor array was quite worn out from the intensive use. Most of polymer coating materials lost some of their initial properties after many adsorption-desorption cycles. The best indication of the exhaustion of some coatings were higher baselines, which are the responses to the “empty” samples, i.e., the samples of the dry air that do not contain any chemical vapors, and lower

responses to the samples contain the target chemical vapors. We found out that some polymer coatings could not be completely "refreshed" (brought to the initial state) after the long use. The experimental data of the gaseous mixtures containing toluene vapors (classes 7 through 9) were collected during the last month of the testing when the quality of the sensor was somewhat degraded. We believe that this fact largely contributed to the higher rate of misclassification of the toluene containing data in some cases. Therefore, we did not consider the data items of class 7 through 9 to be completely reliable to make any judgment about the algorithm's performance and used those data very sparsely for the algorithm's performance evaluation.

We ran a large number of tests in which feature vectors from the different combinations of classes were presented, but in this thesis we used only a few most typical combinations of classes for comparison purposes to illustrate the relative effectiveness and accuracy of the pattern recognition algorithms. In most cases, the complete n-fold cross validation technique was used to evaluate the algorithm's accuracy. We tried to keep the training/testing data set pairs in each case unique as much as possible. If the number of feature vectors belonging to the same class in the data set was large enough, we created testing sets without duplicates between them; otherwise, if the duplicates were unavoidable, we used different combinations of unlabeled feature vectors in each testing set. All testing sets were created in such a way that the number of feature vectors in the testing data set from a specific class is directly proportional to the number of feature vectors with the same label in the combined data set (both training and testing data sets combined together) and all class labels are present in the testing data set. The order of the

feature vectors in both training and testing sets were randomly scrambled in all cases before running the pattern recognition algorithm on those data.

Thus, the results of classification accuracy in each case were calculated as an average over all runs for all training/testing set pairs. In the case of the XCS algorithms, in addition to that, the results of classification accuracy were averaged over 30 different program runs (30 different seeds to randomize the pseudo-random number generator) for each training/testing pair of the data sets.

Table 12 shows the information on the training/testing sets created for the testing experiments in this thesis:

Table 12. Information about training/testing set pairs for algorithm's accuracy evaluation.

Test Number	Class Labels Presented in the Set	Total Number of Vectors	Number of Labeled/Unlabeled Vectors Used in Each Test
1	1, 4	18	(1) 12/6; (2) 12/6; (3) 12/6
2	1, 4, 7	29	(1) 19/10; (2) 19/10; (3) 20/9
3	2, 4, 7	47	(1) 35/12; (2) 35/12; (3) 35/12; (4) 34/13
4	1, 2, 4, 5	53	(1) 42/11; (2) 42/11; (3) 43/10; (4) 43/10
5	1, 2, 3, 4, 5, 6	66	(1) 50/16; (2) 50/16; (3) 49/17; (4) 49/17
6	1, 3, 4, 6, 7, 9	47	(1) 31/16; (2) 31/16; (3) 32/15; (4) 32/15
7	1, 2, 3, 4, 5, 6, 7, 8, 9	85	(1) 64/21; (2) 64/21; (3) 64/21; (4) 63/22

.

5.1 Extended Classifier System (XCS)

The poor performance of the XCS algorithm using our experimental sensory data came as no surprise (see Table 13). We can observe how classification accuracy has been constantly dropping as the number of possible classes in the data set increases.

Table 13. The results of classification accuracy of the XCS algorithm using the cantilever sensor array data.

Test Number	Class Labels Presented in the Set	Classification Accuracy (%)	
		average of max	average of average
1	1, 4	75.555	64.815
2	1, 4, 7	46.556	36.099
3	2, 4, 7	53.184	41.309
4	1, 2, 4, 5	43.485	29.765
5	1, 2, 3, 4, 5, 6	28.217	22.702
6	1, 3, 4, 6, 7, 9	31.488	21.964
7	1, 2, 3, 4, 5, 6, 7, 8, 9	14.286	9.470

There are two main reasons for such low classification accuracy of XCS in the case of our sensory data.

The first reason for that is a small number of feature vectors in the training set. This algorithm was originally designed to learn on a sufficiently large number of the input vectors. As we found out testing this algorithm on the benchmark data sets, in order to reach the peak of its ability to classify a new input vector highly accurate, the population of classifiers of XCS should contain a large number of very experienced

classifiers, where the number of input vectors Q should be much greater than the number of features N in each vector, $Q >> N$. This condition is obviously not possible without a sufficiently large training data set.

The second reason for low classification of XCS is the way we used to encode the feature values into the binary numbers, that is we used only one bit to encode each number n: if $n < 0.5$, then use 0; otherwise, use 1 to encode that number. There is hope that by increasing of a number of bits that are used to encode each feature value into a binary number, we can increase the accuracy of each classifier in the system, hence increase the classification accuracy of the XCS algorithm as a whole.

5.2 Radial Basis Function Neural Network (RBF NN)

Just slightly better were the results of classification accuracy of the RBF NN algorithm on the cantilever sensor array experimental data (see Table 14). The reasons for its poor performance are similar to those of the XCS algorithm: a small number of training set compare to the high vector dimensionality and a relatively large number of different classes in the data set compared to the total number of the feature vectors.

These results are in complete agreement with our initial assumption that the conventional neural network algorithms are not quite suitable for use with the cantilever sensor array data, when the pattern recognition algorithm should be able to extract all needed information about the data from a considerably small number of the exemplar vectors.

Table 14. The results of classification accuracy of the RBF NN algorithm using the cantilever sensor array data.

Test Number	Class Labels Presented in the Set	Classification Accuracy (%)	
		max	average
1	1, 4	50.000	50.000
2	1, 4, 7	55.560	41.853
3	2, 4, 7	58.330	55.285
4	1, 2, 4, 5	50.000	35.908
5	1, 2, 3, 4, 5, 6	37.500	33.363
6	1, 3, 4, 6, 7, 9	26.670	24.168
7	1, 2, 3, 4, 5, 6, 7, 8, 9	28.570	27.055

5.3 Support Vector Machines (SVMs)

Traditionally, the SVM algorithm is considered to be the best performer among other pattern recognition algorithms for the data sets that contain a small number of the highly dimensional feature vectors.

However, as we can see from the testing results provided below (Table 15, Table 16, and Table 17), the SVM algorithm performs well only on the data from the limited number of classes. Once the diversity of the feature vectors in the same data set increases, classification accuracy of the SVM algorithm drops (sometimes significantly). Even though the Gaussian kernel is typically considered to be the best choice for the kernel, in our case the best classification accuracy was obtained with the use of the simplest kernel function, the linear kernel.

Table 15. The results of classification accuracy of the SVM algorithm with the Gaussian kernel using the cantilever sensor array data.

Gaussian kernel: $k^{(g)}(\vec{x},\vec{s}^{(i)}) = \exp\left(-\frac{\| \vec{x}-\vec{s}^{(i)} \|^2}{\gamma}\right)$			
Test Number	Class Labels Presented in the Set	Classification Accuracy (%)	
		max	average
1	1, 4	100.000	100.000
2	1, 4, 7	100.000	100.000
3	2, 4, 7	100.000	100.000
4	1, 2, 4, 5	63.636	61.818
5	1, 2, 3, 4, 5, 6	64.706	63.603
6	1, 3, 4, 6, 7, 9	80.000	71.250
7	1, 2, 3, 4, 5, 6, 7, 8, 9	61.905	58.875

Table 16. The results of classification accuracy of the SVM algorithm with the linear kernel using the cantilever sensor array data.

Linear kernel: $k^{(l)}(\vec{x}, \vec{s}^{(i)}) = \vec{x} \cdot \vec{s}^{(i)}$			
Test Number	Class Labels Presented in the Set	Classification Accuracy (%)	
		max	average
1	1, 4	100.000	100.000
2	1, 4, 7	100.000	100.000
3	2, 4, 7	100.000	100.000
4	1, 2, 4, 5	81.818	78.409
5	1, 2, 3, 4, 5, 6	88.235	86.397
6	1, 3, 4, 6, 7, 9	100	98.333
7	1, 2, 3, 4, 5, 6, 7, 8, 9	85.714	82.413

Table 17. The results of classification accuracy of the SVM algorithm with the polynomial of degree 3 kernel using the cantilever sensor array data.

Polynomial kernel: $k^{(p)}(\vec{x},\vec{s}^{(i)}) = (1+\vec{x}\cdot\vec{s}^{(i)})^3$			
Test Number	Class Labels Presented in the Set	Classification Accuracy (%)	
		max	average
1	1, 4	100.000	100.000
2	1, 4, 7	100.000	100.000
3	2, 4, 7	100.000	100.000
4	1, 2, 4, 5	81.818	80.909
5	1, 2, 3, 4, 5, 6	76.471	74.265
6	1, 3, 4, 6, 7, 9	80.000	77.500
7	1, 2, 3, 4, 5, 6, 7, 8, 9	71.429	68.236

Surprisingly, the SVM algorithm, despite its high reputation of being the best pattern recognition algorithm for the compact data sets with high dimensional feature vectors, did not come up to our expectations for the multi-class data.

5.4 Fuzzy Neural Network (FNN)

Even though the FNN algorithm is the simplest among all pattern recognition algorithms that had been used in the current research, it performed extremely well on our cantilever sensor array data (see Table 18 and Table 19). We expected this algorithm to be highly accurate on data that are not noisy and do not contain outliers, but the fact that the FNN algorithm is doing so well on quite compact data sets that contain the feature vectors from the large pool of different classes was quite surprising.

Table 18. The results of classification accuracy of the FNN algorithm with the discriminant function f^1 using the cantilever sensor array data.

$f_j^1(\vec{x}) = \{\max\{k(\vec{x}, \vec{x}^{(q_j)}) : q_j = 1,...,Q_j\}$			
Test Number	Class Labels Presented in the Set	Classification Accuracy (%)	
		max	average
1	1, 4	100.000	100.000
2	1, 4, 7	100.000	100.000
3	2, 4, 7	100.000	100.000
4	1, 2, 4, 5	100.000	92.728
5	1, 2, 3, 4, 5, 6	100.000	92.463
6	1, 3, 4, 6, 7, 9	100.000	96.770
7	1, 2, 3, 4, 5, 6, 7, 8, 9	95.240	87.230

Table 19. The results of classification accuracy of the FNN algorithm with the discriminant function f^2 using the cantilever sensor array data.

$f_j^2(\vec{x}) = \frac{1}{Q_j}\sum_{q_j=1}^{Q_j} k(\vec{x}, \vec{x}^{(q_j)})$			
Test Number	Class Labels Presented in the Set	Classification Accuracy (%)	
		max	average
1	1, 4	100.000	100.000
2	1, 4, 7	100.000	100.000
3	2, 4, 7	100.000	100.000
4	1, 2, 4, 5	100.000	90.228
5	1, 2, 3, 4, 5, 6	100.000	90.993
6	1, 3, 4, 6, 7, 9	100.000	96.770
7	1, 2, 3, 4, 5, 6, 7, 8, 9	95.240	88.365

5.5 Fuzzy Classifier based on Fuzzy *C*-Means Clustering (FCM-based)

As we predicted based on the benchmark data sets testing, the fuzzy classifier based on the FCM algorithm performed very well on our sensory data (see Table 20 and Table 21). Its classification accuracy is similar to our FNN algorithm. Even though this algorithm is more complex than FNN, we believe that it is more reliable in a broader range of situations, for example in the case of outliers and mislabeled samples, since it allows us to easily locate such data and exclude those samples from the classification phase.

Table 20. The results of classification accuracy of the fuzzy classifier based on FCM-based algorithm with the discriminant function f^1 using the cantilever sensor array data.

$f_j^1(\vec{x}) = k(\vec{x}, \vec{v}^{(j)})$			
Test Number	Class Labels Presented in the Set	Classification Accuracy (%)	
		max	average
1	1, 4	100.000	100.000
2	1, 4, 7	100.000	100.000
3	2, 4, 7	100.000	100.000
4	1, 2, 4, 5	100.000	87.728
5	1, 2, 3, 4, 5, 6	100.000	88.143
6	1, 3, 4, 6, 7, 9	100.000	96.668
7	1, 2, 3, 4, 5, 6, 7, 8, 9	90.480	85.875

Table 21. The results of classification accuracy of the fuzzy classifier based on FCM-based algorithm with the discriminant function f^2 using the cantilever sensor array data.

$f_j^2(\vec{x}) = \max\{k(\vec{x}, \vec{x}^{(q_j)}) : q_j = 1,...,Q_j\}$			
Test Number	Class Labels Presented in the Set	Classification Accuracy (%)	
		max	average
1	1, 4	100.000	100.000
2	1, 4, 7	100.000	100.000
3	2, 4, 7	100.000	100.000
4	1, 2, 4, 5	100.000	95.000
5	1, 2, 3, 4, 5, 6	93.750	89.523
6	1, 3, 4, 6, 7, 9	100.000	96.668
7	1, 2, 3, 4, 5, 6, 7, 8, 9	90.480	85.875

5.6 Fuzzy Classifier based on Fuzzy Connectivity Clustering (FCC-based)

Table 22 and Table 23 show the results of classification accuracy of the FCC algorithm. As expected, based on its intrinsic properties and recent improvements, FCC performed the best among all pattern recognition algorithms on our sensory data.

Table 22. The results of classification accuracy of the semi-supervised version of the FCC-based algorithm using the cantilever sensor array data.

Semi-supervised Clustering (Short Version): labeled and unlabeled feature vectors are clustered together			
Test Number	Class Labels Presented in the Set	Classification Accuracy (%)	
		max	average
1	1, 4	100.000	96.667
2	1, 4, 7	100.000	97.917
3	2, 4, 7	100.000	100.000
4	1, 2, 4, 5	100.000	100.000
5	1, 2, 3, 4, 5, 6	100.000	92.463
6	1, 3, 4, 6, 7, 9	100.000	93.542
7	1, 2, 3, 4, 5, 6, 7, 8, 9	95.238	87.175

Table 23. The results of classification accuracy of the full version of the FCC-based algorithm that clustered labeled vectors separately from unlabeled ones using the cantilever sensor array data.

Unsupervised Clustering (Full Version): labeled feature vectors are clustered separately from unlabeled			
Test Number	Class Labels Presented in the Set	Classification Accuracy (%)	
		max	average
1	1, 4	100.000	100.000
2	1, 4, 7	100.000	100.000
3	2, 4, 7	100.000	100.000
4	1, 2, 4, 5	100.000	100.000
5	1, 2, 3, 4, 5, 6	100.000	97.059
6	1, 3, 4, 6, 7, 9	100.000	95.000
7	1, 2, 3, 4, 5, 6, 7, 8, 9	100.000	90.639

6 Conclusion and Future Work

Within the framework of the current research several objectives have been achieved.

It has been found that the information extracted from just the resonance frequency shifts of cantilever sensors in the microfabricated array during exposure of the array to the target analyte vapors is mostly sufficient for creating fingerprints of the analytes. The measured resonance frequency shift responses of the cantilevers can be used as an input to the variety of pattern recognition algorithms for the purpose of creating a reliable system that is capable of detecting and recognizing a variety of target analytes and quantitative estimation of the relative concentration of those analyte vapors in a gaseous mixture, for example in the ambient air.

During the multiple experiments with microfabricated cantilever sensors it has been demonstrated that the use of the array of cantilevers with some of cantilevers being functionalized by coating their surface with thoroughly chosen commercial polymers has significantly improved the selectivity of the sensor array as a whole to the target analytes.

As a result of experimental work, the cantilever resonance frequency responses during exposure of the array of cantilever sensors to the dry air and the air containing different concentration (*high* – 26%, *medium* – 18%, and *low* – 7%) of vapors of the three different organic solvents: acetone, ethanol, and toluene, have been collected.

After careful examination, the procedure of extracting the most important information out of 7000 different measurements for each sample has been created. By

applying the created strategy for feature extraction, the data set of 34-dimensional feature vectors has been created.

The main goal of the current research was to create pattern recognition algorithms that can be effectively used as a reliable detection system with the specific sensory data obtained during the experiments with a microfabricated cantilever sensor array and further feature extracting procedure.

Five different pattern recognition algorithms have been created for the current research. All of those algorithms and the open source implementation of the sixth algorithm (multiclass SVMs) were used for testing on benchmark data sets and collected sensory data. It has been shown that the kernel-based algorithms have the greatest potential to be used with the microfabricated cantilever sensor array in the detection systems. Four out of six pattern recognition algorithms have produced high accuracy classification results upon processing the cantilever sensor array data.

Despite the fact that the extended classifier system (XCS) algorithm showed quite a good performance on the benchmark data sets, it failed to produce equally good classification results on our sensory data. Even though we believe that XCS could be successfully modified to accommodate specific properties of the sensory data, especially a very small size of the data set and high dimensionality of the feature vectors, in order to increase its classification accuracy, we do not consider this algorithm as a good choice for the cantilever sensor array detection system.

It has been also shown that the radial basis function neural network (RBF NN) algorithm is not especially effective in the case of small training data sets, high

dimensionality of the feature vectors, and multiclass environment. We believe that further attempts to employ the neural networks as a pattern recognition algorithm to be used with a microcantilever sensor array for detection, recognition, and quantitative estimation of the target analytes do not hold considerable promise.

The SVM algorithm has a solid reputation of being the best performer in the case of the limited number of high dimensional feature vectors available for training. However, this algorithm is very sensitive to the noisy data and outliers. Since the sensory data are prone to suffer from noise and a variety of reading device errors, the SVM algorithm cannot be one hundred percent reliable in every situation that may be encountered during the detection process. Besides, it has been demonstrated that the classification accuracy of the SVM algorithm dropped significantly with the increase of the number of different classes in the limited experimental data. However, in many cases, SVM still might provide satisfying results and therefore, can be cautiously used as a part of the detection system.

Fuzzy logic and the notion of fuzziness provide a useful framework for representing uncertainty in the sensory data. It has been shown that the fuzzy approach to creating a reliable classifier system is particularly relevant for the cantilever sensor array data. The fuzzy neural network (FNN) algorithm that is essentially the kernel-based fuzzy classifier has produced the excellent results on the cantilever sensor array data. This algorithm is very simple and asymptotically very efficient. In the case of absence of the outliers and mislabeled samples, it should be the first choice for the pattern recognition algorithm to be used with sensory data.

However, the noisy data and outliers are quite common among the cantilever sensor array data. In this thesis it has been shown that a combination of a clustering analysis, as a pre-processing technique, and a fuzzy classifier creates a powerful tool for the simultaneous, accurate, fast, more reliable and robust detection and identification of the target analytes in a gaseous mixture with the use of a microcantilever sensor array.

The combination of unsupervised and semi-supervised data analysis of the labeled training data set allows identifying the outliers and mislabeled data and creating a basis for the highly precise fuzzy classifiers to be used for unseen before data samples. It has been determined that fuzzy classifiers based on the fuzzy *c*-means clustering and fuzzy connectivity clustering algorithms clearly outperformed the traditionally used neural networks and in some cases even the SVM algorithm and could be considered as the most promising pattern recognition algorithms to be used with the microcantilever sensor array as a selective and quantitative chemical detection system.

Thus, in this thesis it has been demonstrated that a micromechanical array of cantilever sensors can be used in combination with the certain types of pattern recognition algorithms to examine the gaseous mixtures and detect target analytes with high accuracy (100% in most cases). A combination of a clustering analysis and fuzzy classifiers creates a family of powerful pattern recognition algorithms for the cantilever sensor array data. In the case of consistent and noiseless sensory data FNN could be the best choice for the pattern recognition algorithm.

Future work needs to be focused on the further modification of the mentioned above kernel-based fuzzy classifier algorithms as a part of the detection systems. There

are some useful features that can be easily incorporated into those algorithms. For example, 1) the automatic detection of the noisy data and outliers and removing them from the training data sets, and 2) calculating the standard deviation of a cluster based on the density of the feature vectors in it, instead of the averaged distances between feature vectors and a center of the cluster.

Another research area that should be given close attention is an analysis of the analyte mixtures. The preliminary test results with binary mixtures of acetone and ethanol vapors obtained during the current research are highly supportive of the idea that these pattern recognition algorithms are precisely the right method for the detection, identification, and quantitative estimation of every component in the complex mixtures of the target analytes, even in the absence of exhaustive training data. Therefore, more studies have to be done in that direction as well. This ability to successfully analyze analytes' mixtures will greatly increase the range of classification of the detection system and help to meet increasing demand for such systems.

7 Appendices

7.1 Appendix A – Implementation Details of XCS Algorithm

The XCS classifier system has been fully implemented in C++ using the object-oriented approach. For this purpose, five classes have been created:

1. Class *Counter* – responsible for creating a unique identification number for each classifier as well as for keeping track of the total number of the GA performed.
2. Class *Clock* – responsible for time stamping each classifier at birth and updating the time-stamp every time the classifier happens to be in [*A*] during the GA. This class also keeps track of the time when explore approach in selecting the action in [*A*] has been used.
3. Class *Input* – responsible for creating input strings to send to the classifier systems and all operation related to the input.
4. Class *Classifier* – responsible for creating classifiers, as well as for all operation related to the classifiers.
5. Class *XCS* – responsible for creating the entire classifier system that contains members of both *Input* and *Classifier* classes (along with the others) and running the algorithm throughout the entire experiment.

Table 24. A list of important parameters and their values used in the current implementation.

Parameter	Value	Description
N_{init}	100	Initial population size
N_{max}	500	Maximum population size
θ_{mna}	4	Minimum number of classifiers that [*M*] should contain before forming [*A*]; otherwise covering occurs
β	0.2	Learning rate for prediction, prediction error, fitness, and estimate of the size of [*A*] update
γ	0.71	Discounting factor for calculating the total Reward (used only for multi-step problems)
θ_{ga}	25	Do GA if the average time since the last GA exceeds this threshold
α	0.1	Parameter for calculating the error function
ε_0	5.0	Parameter for calculating the error function
ν	4.4	Parameter for calculating the error function
χ	0.8	Probability of Crossover
μ	0.04	Probability of Mutation
$P_{\#}$	0.33	Probability of "Don't Care"
δ	0.1	Value of a fraction used in the deletion scheme
p_I	100.0	Initial value of prediction (set at birth)
ε_I	10.0	Initial value of prediction error (set at birth)
F_I	0.01(×1000)	Initial value of fitness (set at birth)
EE	600	Exploration experience
$rate_1$	50	Exploration rate 1
$rate_2$	10	Exploration rate 2

$rate_3$	5	Exploration rate 3
$rate_4$	2	Exploration rate 4
NM	8	Niche mutation rate
DE	15	Deletion experience
SE	20	Subsumption experience

7.2 Appendix B – Implementation Details of FCC Algorithm

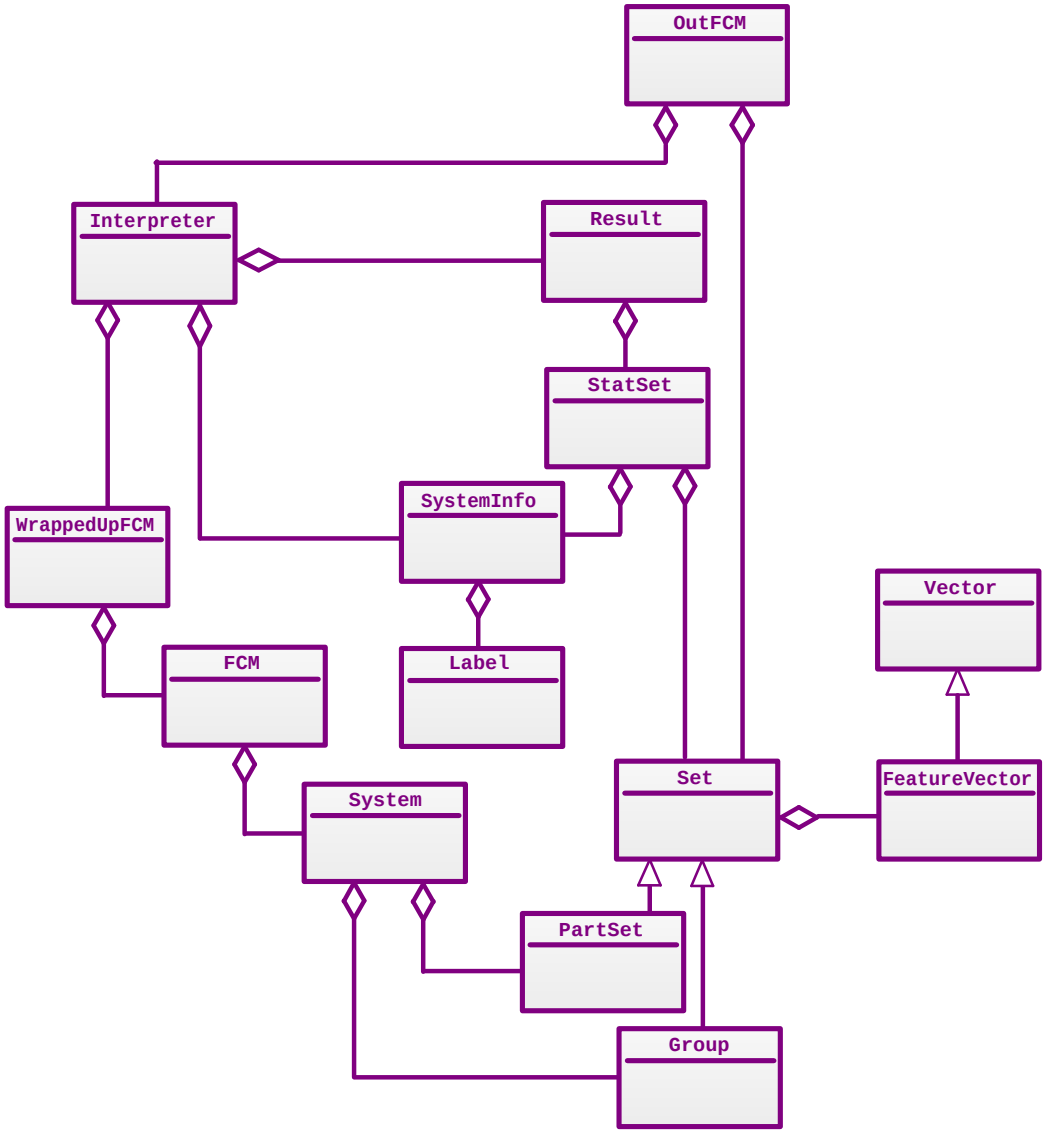

Figure 22. Class diagram of the OOP implementation of the FCC algorithms.

8 References

[1] S. Zaromb and J.R. Stetter, "Theoretical basis for identification and measurement of air contaminants using an array of sensors having partly overlapping selectivities," *Sensors and Actuators*, vol. 6(4), pp. 225−243, 1984.

[2] H. Abe, T. Yoshimura, S. Kanaya, Y. Takahashi, Y. Miyashita, and S.-I. Sasaki, "Automated odor-sensing system based on plural semiconductor gas sensors and computerized pattern recognition techniques," *Analytica Chimica Acta*, vol. 194, pp. 1−9, 1987.

[3] H. Abe, S. Kanaya, Y. Takahashi, and S.-I. Sasaki, "Extended studies of the automated odor-sensing system based on plural semiconductor gas sensors with computerized pattern recognition techniques," *Analytica Chimica Acta*, vol. 215, pp. 155−168, 1988.

[4] T. Thundat, P.I. Oden, and R.J. Warmack, "Microcantilever Sensors," *Microscale Thermophysical Engineering*, vol. 1(3), pp. 185−199, 1997.

[5] N. Abedinov, C. Popov, Zh. Yordanov, Tzv. Ivanov, T. Gotszalk, P. Grabiec, W. Kulisch, I.W. Rangelow, D. Filenko, and Yu. Shirshov, "Chemical recognition based on micromachined silicon cantilever array," *J. Vacuum Science & Technology: B*, vol. 21(6), pp. 2931−2936, 2003.

[6] N.V. Lavrik, M.J. Sepaniak, P.G. Datskos, "Cantilever transducers as a platform for chemical and biological sensors," *Review of Scientific Instruments*, vol. 75(7), pp. 2229−2953, 2004.

[7] H.P. Lang, M. Hegner and Ch. Gerber, “Microfabricated Cantilever Array Sensors for (Bio-)Chemical Detection,” In: B. Bhushan and H. Fuchs (Eds.), “Applied Scanning Probe Methods IV – Industrial Applications,” Springer-Verlag, Berlin, New York, Heidelberg, Chapter 28, pp. 183−213, 2006.

[8] J.W. Grate and D.A. Nelson, “Sorptive polymeric materials and photopatterned films for gas phase chemical microsensors,” *Proc. IEEE*, vol. 91(6), pp. 881−889, 2003.

[9] R. Gutierrez-Osuna, “Pattern analysis for machine olfaction: a review,” *IEEE Sensors Journal*, vol. 2(3), pp. 189–202, 2002.

[10] G. Binning, C. F. Quate, and Ch. Gerber, “Atomic Force Microscope,” *Physical Review Letters*, vol. 56(9), pp. 930–933, 1986.

[11] H.P. Lang, M. Hegner, Ch. Gerber, "Cantilever Array Sensors,” *Materials Today*, vol. 8(4), pp. 30–36, 2005.

[12] R. Berger, E. Delamarche, H.P. Lang, C. Gerber, J.K. Gimzewski, E. Meyer, and H.-J. Güntherodt, “Surface Stress in the Self-Assembly of Alkanethiols on Gold,” vol. 276(5321), *Science*, pp. 2021–2024, 1997.

[13] J. Fritz, M.K. Baller, H.P. Lang, H. Rothuizen, P. Vettiger, E. Meyer, H.-J. Güntherodt, Ch. Gerber, and J.K. Gimzewski, “Translating Biomolecular Recognition into Nanomechanics,” *Science*, vol. 288(5464), pp. 316–318, 2000.

[14] J.P. Cleveland, S. Manne, D. Bocek, P.K. Hansma, “A nondestructive method for determining the spring constant of cantilevers for scanning force microscopy,” *Review of Scientific Instruments*, vol. 64(2), pp. 403–405, 1993.

[15] T. Thundat, R.J. Warmack, ”Thermal and ambient-induced deflections of scanning force microscope cantilevers,” *Applied Physics Letters*, vol. 64(21), pp. 2894–2896, 1994.

[16] E.A. Wachter, T. Thundat, “Micromechanical sensors for chemical and physical measurements,” *Review of Scientific Instruments*, vol. 66(6), pp. 3662–3667, 1995.

[17] J.W. Grate, “Acoustic Wave Microsensor Arrays for Vapor Sensing,” *Chemical Reviews*, vol. 100(7), pp. 2627–2648, 2000.

[18] E.T. Zellers, S.A. Batterman, M. Han, S.J. Patrash, , “Optimal coating selection for the analysis of organic vapor mixtures with polymer-coated surface acoustic wave sensor arrays,” *Analytical Chemistry*, vol. 67 (6), pp. 1092–1106, 1995.

[19] M.P. Eastman, R.C. Hughes, G. Yelton, A.J. Ricco, S.V. Patel, and M.W. Jenkins, “Application of the Solubility Parameter Concept to the Design of Chemiresistor Arrays,” *Journal of the Electrochemical Society*, vol. 146(10), pp. 3907–3913, 1999.

[20] F. Bender, L. Wachter, A. Voigt, and M. Rapp, “Deposition of high quality coatings on SAW sensors using electrospray,” *Proc. Second Int. IEEE Conf. Sensors*, vol. 1, pp. 115–119, 2003.

[21] S. Sarkar, N. Levit, and G. Tepper, “Deposition of polymer coatings onto SAW resonators using AC electrospray,” *Sensors and Actuators B*, vol. 114(2), pp. 756–761, 2006.

[22] A. Bietsch, J. Zhang, M. Hegner, H.P. Lang, and C. Gerber, "Rapid functionalization of cantilever array sensors by inkjet printing," *Nanotechnology*, vol. 15(8), pp. 873–880, 2004.

[23] S. Alexander, L. Hellemans, O.Marti, J. Schneir, V. Elings, P.K. Hansma,M. Longmire, and J. Gurley, "An atomic-resolution atomic-force microscope implemented using an optical lever," *Journal of Applied Physics*, vol. 65(1), pp. 164–167, 1989.

[24] E.A. Wachter, T. Thundat, P.I. Oden, R.J. Warmack, P.G. Datskos, and S.L. Sharp, "Remote optical detection using microcantilevers," *Review of Scientific Instruments*, vol. 67(10), pp. 3434–3439, 1996.

[25] M. Tortonese, R.C. Barrett, and C.F. Quate, "Atomic resolution with an atomic force microscope using piezoresistive detection," *Applied Physics Letters*, vol. 62(8), pp. 834–836, 1993.

[26] T.L. Porter, M.P. Eastman, D.L. Pace, and M. Bradley, "Sensor based on piezoresistive microcantilever technology," *Sensors and Actuators A*, vol. 88(1), pp. 47–51, 2001.

[27] S.A. Miller**,** K.L. Turner**,** N.C. MacDonald, "Microelectromechanical scanning probe instruments for array architectures," *Review of Scientific Instruments*, vol. 68(11), pp. 4155–4162, 1997.

[28] K. K. Park, H. J. Lee, G. G. Yaralioglu, A. S. Ergun, Ö. Oralkan, M. Kupnik, C. F. Quate, and B. T. Khuri-Yakub, T. Braun, J.-P. Ramseyer, H. P. Lang, M. Hegner, Ch. Gerber, and J. K. Gimzewski, "Capacitive micromachined ultrasonic

transducers for chemical detection in nitrogen," *Applied Physics Letters*, vol. 91(9), pp. 094102-1–094102-3, 2007.

[29] D.L. DeVoe, and A.P. Pisano, "Modeling and optimal design of piezoelectric cantilever microactuators," *Journal of Microelectromechanical Systems*, vol. 6(3), pp. 266–270, 1997.

[30] T. Itoh, C. Lee, T. Suga, "Deflection detection and feedback actuation using a self-excited piezoelectric $Pb(Zr,Ti)O_3$ microcantilever for dynamic scanning force microscopy," *Applied Physics Letters*, vol. 69(14), pp. 2036–2038, 1997.

[31] S. Zurn, M. Hsieh, G. Smith, D. Markus, M. Zang, G. Hughes, Y. Nam, M. Arik, and D. Polla "Fabrication and structural characterization of a resonant frequency PZT microcantilever," *Smart Materials and Structures*, vol. 10(2), pp. 252–263, 2001.

[32] J. D. Adams, G. Parrott, C. Bauer, T. Sant, L. Manning, M. Jones, B. Rogers, D. McCorkle, and T. L. Ferrell, "Nanowatt chemical vapor detection with a self-sensing, piezoelectric microcantilever array," *Applied Physics Letters*, vol. 83(16), pp. 3428–3430, 2003.

[33] J. Park, W.A. Groves, and E.T. Zellers, "Vapor Recognition with Small Arrays of Polymer-Coated Microsensors. A Comprehensive Analysis," *Analytical Chemistry*, vol. 71(17), pp. 3877–3886, 1999.

[34] M.K. Baller, H.P. Lang, J. Fritz, Ch. Gerber, J.K. Gimzewski, U. Drechsler, H. Rothuizen, M. Despont, P. Vettiger, F.M. Battiston, J.P. Ramseyer, P. Fornaro, E.

Meyer, H.-J. Güntherodt, "A cantilever array-based artificial nose," *Ultramicroscopy*, vol. 82(1), pp. 1–9, 2001.

[35] H.P. Lang, J.P. Ramseyer, W. Grange, T. Braun, D. Schmid, P. Hunziker, C. Jung, M. Hegner, and C. Gerber, "An Artificial Nose Based on Microcantilever Array Sensors," *Journal of Physics: Conference Series*, vol. 61, pp. 663–667, 2007.

[36] M. Penza and G. Cassano, "Application of principal component analysis and artificial neural networks to recognize the individual VOCs of methanol/2-propanol in a binary mixture by SAW multi-sensor array," *Sensors and Actuators B*, vol. 89(3), pp. 269–284, 2003.

[37] W.P. Carey, K.R. Beebe, B.R. Kowalski, D.L. Illman, and T. Hirschfeld "Selection of adsorbates for chemical sensor arrays by pattern recognition," *Analytical Chemistry*, vol. 58(1), pp. 149–153, 1986.

[38] L.R. Senesac, P. Dutta, P.G. Datskos, and M.J. Sepaniak, "Analyte species and concentration identification using differentially functionalized microcantilever arrays and artificial neural networks," *Analytica Chimica Acta*, vol. 558, pp. 94–101, 2006.

[39] S.-M. Chang, Y. Iwasaki, M. Suzuki, E. Tamiya, I. Karube, and H. Muramatsu "Detection of odorants using an array of piezoelectric crystals and neural-network pattern recognition," *Analytica Chimica Acta*, vol. 249(2), pp. 323–329, 2001.

[40] C.D. Natale, F.A.M. Davide, A. D'Amico, A. Hierlemann, J. Mitrovics, M. Schweizer, U. Weimar, and W. Göpel, "A composed neural network for the

recognition of gas mixtures," *Sensors and Actuators B*, vol. 24-25, pp. 808–812, 1995.

[41] B.H. Kim, F.E. Prins, D.P. Kern, S. Raible, and U. Weimar, "Multicomponent analysis and prediction with a cantilever array based gas sensor," *Sensors and Actuators B*, vol. 78(1), pp. 12–18, 2001.

[42] D. Then, A. Vidic, and Ch. Ziegler, "A highly sensitive self-oscillating cantilever array for the quantitative and qualitative analysis of organic vapor mixtures," *Sensors and Actuators B*, vol. 117(1), pp. 1–9, 2006.

[43] G. Barkó, J. Abonyi, and J. Hlavay, "Application of fuzzy clustering and piezoelectric chemical sensor array for investigation on organic compounds." Available at <http://www.fmt.vein.hu/softcomp/Abonyi99-AnalChim.pdf>. Last accessed on Oct 27 2007.

[44] M. Kermit and O. Tomic, "Independent Component Analysis Applied on Gas Sensor Array Measurement Data," *IEEE Sensors Journal*, vol. 3(2), pp. 218v228, 2003.

[45] R. Archibald, P. Datskos, G. Devault, V. Lamberti, N. Lavrik, D. Noid, M. Sepaniak, and P. Dutta, "Independent component analysis of nanomechanical responses of cantilever arrays," *Analytica Chimica Acta*, vol. 584, pp. 101–105, 2007.

[46] M. Wang, A. Perera, and R. Gutierrez-Osuna "Principal Discriminants Analysis for small-sample-size problems: application to chemical sensing," *Proc. 3rd IEEE Conf. Sensors*, Vienna, Austria, 2004.

[47] R.O. Duda, P.E. Hart, and D.G. Stork, "Pattern Classification," 2nd Ed., Willey-Interscience, New York, 2001.

[48] I.T. Jolliffe, "Principal Component Analysis," 2nd Ed., Springer-Verlag, New York, 2002.

[49] G.J. McLachlan, "Discriminant Analysis and Statistical Pattern Recognition," Wiley-Interscience, New York, 2004.

[50] D.F. Specht, **"**Probabilistic neural networks for classification, mapping, or associative memory," *IEEE Int. Conf. Neural Networks*, vol. 1, pp. 525–532, 1988.

[51] D.F. Specht, **"**Enhancements to probabilistic neural networks," *IEEE Int. Joint Conf. Neural Networks*, vol. 1, pp. 761–768, 1992.

[52] A. Zaknich, and C.J.S. de Silva, "Adaptive learning schemes for the modified probabilistic neural network," *3rd Int. Conf. Algorithms and Architectures for Parallel Processing*, pp. 597–610, 1997.

[53] Z.R. Yang, and S. Chen, "Robust maximum likelihood training of heteroscedastic probabilistic neural networks," *Neural Networks*, vol. 11(4), pp. 739–747, 1998.

[54] L. Rutkowski, "Adaptive probabilistic neural networks for pattern classification in time-varying environment," *IEEE Trans. Neural Networks*, vol. 15(4), pp. 811–827, 2004.

[55] J. Moody and C. J. Darken, "Fast learning in networks of locally-tuned processing units," *Neural Computation,* vol. 1(2), pp. 281–294, 1989.

[56] T. Poggio and F. Girosi, "Networks for approximation and learning," *Proc. IEEE*, vol. 78(9), pp. 1481–1497, 1990.

[57] S.V.T. Elanayar, Y.C. Shin, "Radial basis function neural network for approximation and estimation of nonlinear stochastic dynamic systems," *IEEE Trans. Neural Networks*, vol. 5(4), pp. 594–603, 1994.

[58] F. Anouar, F. Badran and S. Thiria, "Probabilistic self-organizing map and radial basis function," *Neurocomputing*, vol. 20, pp. 83–96, 1998.

[59] Z.R. Yang, "A novel radial basis function neural network for discriminant analysis," *IEEE Trans. Neural Networks*, vol. 17(3), pp. 604–612, 2006.

[60] A.K. Jain and R.C. Dubes, "Algorithms for Clustering Data," Prentice-Hall, Englewood Cliffs, New Jersey, 1988.

[61] A.K. Jain, M.N. Murty, and P.J. Flynn, "Data clustering: a review," *ACM Computing Surveys*, vol. 31(3), pp. 264–323, 1999.

[62] J.C. Bezdek and S.K. Pal (Eds), "Fuzzy Models for Pattern Recognition: Methods that Search for Structures in Data," IEEE Press, New York, 1992.

[63] A. Baraldi and P. Blonda, "A survey of fuzzy clustering algorithms for pattern recognition – Part I," *IEEE Trans. Systems, Man, and Cybernetics – Part B: Cybernetics*, vol. 29(6), pp. 778–785, 1999.

[64] A. Baraldi and P. Blonda, "A survey of fuzzy clustering algorithms for pattern recognition – Part II," *IEEE Trans. Systems, Man, and Cybernetics – PartB: Cybernetics*, vol. 29(6), pp. 786–801, 1999.

[65] V.N. Vapnik, The Nature of Statistical Learning Theory, Springer, New York, Inc., New York, NY, USA, 1995.

[66] N. Cristianini and J. Shawe-Taylor, "An Introduction to Support Vector Machines," Cambridge University Press, Cambridge, 2000.

[67] B. Schölkopf and A.J. Smola, "Learning with Kernels: Support Vector Machines, Regularization, Optimization, and Beyond," The MIT Press, Cambridge, MA, 2002.

[68] C. Campbell, "Kernel methods: a survey of current techniques," *Neurocomputing*, vol. 48, pp. 63–84, 2002.

[69] V.D. Sánchez A., "Advanced support vector machines and kernel methods," *Neurocomputing*, vol. 55, pp. 5–20, 2003.

[70] J.H. Holland and J.S. Reitman, "Cognitive systems based on adaptive algorithms," In: D.A. Waterman and F. Hayes-Roth (Eds.), "Pattern directed inference systems," Saunders College Publishing, Harcourt Brace, 1978.

[71] J.H. Holland, "Escaping brittleness: The possibilities of general purpose learning algorithms applied to parallel rule-based systems," In: R.S. Michalski, J.G. Carbonell, and T.M. Mitchell (Eds.), "Machine Learning: An artificial intelligence approach, Vol. II," Morgan Kaufmann, Los Altos, CA, 1986.

[72] L.B. Booker, "Triggered Rule Discovery in Classifier Systems," *Proc. 3rd Int. Conf. Genetic Algorithms*, pp. 265-274, 1989.

[73] S.W. Wilson, "ZCS: A Zeroth Level Classifier System," *Evolutionary Computation*, vol. 2(1), pp. 1–18, 1994.

[74] S.W. Wilson, "Classifier fitness based on accuracy," *Evolutionary Computation*, vol. 3(2), pp. 149–177, 1995.

[75] University of California, Irvine. UCI Machine Learning Repository. Available at: <http://mlearn.ics.uci.edu/MLRepository.html> Last accessed on Oct 4 2007.

[76] S.W. Wilson, "Generalization in the XCS Classifier System," *Genetic Programming 1998: Proceedings of the Third Annual Conference*, J. Koza et al. (Eds.), Morgan Kaufmann, San Francisco, CA, pp. 665–674, 1998.

[77] M. Butz, T. Kovacs, P.L. Lanzi, and S.W. Wilson, "Toward a theory of generalization and learning in XCS," *IEEE Trans. Evolutionary Computation*, vol. 8(1), pp. 28-46, 2004.

[78] L.B. Booker, "Intelligent behavior as an adaptation to the task environment," *Ph.D. Dissertation* (Computer and Communication Sciences). The University of Michigan, 1982.

[79] M.V. Butz and S.W. Wilson, "An algorithmic description of XCS," *Advances in Learning Classifier Systems: Proc. 3rd Int. Workshop*, P.L. Lanzi, W. Stolzmann, and S.W. Wilson (Eds.), Springer-Verlag, Berlin, Germany, 2001, *LNAI* pp. 253–272, 1996.

[80] T. Kovacs, "Deletion schemes for classifier systems," *Proc. Genetic and Evolutionary Computation Conf. (GECCO-99)*, W. Banzhaf, J. Daida, et al. (Eds.), San Francisco, CA, pp. 329–336, 1999.

[81] S. Mika, G. Rätsch, J. Weston, B. Schölkopf, and K.-R. Müller, "Fisher discriminant analysis with kernels," in *Neural Networks for Signal Processing IX*, Y.-H. Hu, J. Larsen, E. Wilson, and S. Douglas (Eds.), IEEE, Piscataway, NJ, pp. 41–48, 1999.

[82] G. Baudat and F. Anouar, "Generalized discriminant analysis using a kernel approach," *Neural Computation*, vol. 12(10), pp. 2385–2404, 2000.

[83] B. Schölkopf, A. J. Smola, and K.-R. Müller, "Nonlinear component analysis as a kernel eigenvalue problem," *Neural Computation*, vol. 10(5), pp. 1299–1319, 1998.

[84] A. Ben-Hur, D. Horn, H.T. Siegelmann, and V.N. Vapnik, "A support vector clustering method," *Proc. 15th Int. Conf. Pattern Recognition*, vol. 2, pp. 724–727, 2000.

[85] M. Girolami, "Mercer kernel-based clustering in feature space," *IEEE Trans. Neural Networks*, vol. 13(3), pp. 780–784, 2002.

[86] J.-H. Chiang and P.-Y. Hao, "A New Kernel-Based Fuzzy Clustering Approach: Support Vector Clustering With Cell Growing," *IEEE Trans. Fuzzy Systems*, vol. 11(4), pp. 518–527, 2003.

[87] M. Filippone, F. Camastra, F. Masulli, and S. Rovetta, "A survey of kernel and spectral methods for clustering," *Pattern Recognition*, vol. 41(1), pp. 176-190, 2008.

[88] J. Shawe-Taylor and N. Cristianini, "Kernel Methods for Pattern Analysis," Cambridge University Press, Cambridge, 2004.

[89] C.M. Bishop, "Neural Networks for Pattern Recognition," Oxford University Press, London, U.K., 1995.

[90] C.G. Looney, "Radial basis functional link nets and fuzzy reasoning," *Neurocomputing*, vol. 48, pp. 489–509, 2002.

[91] T. Joachims, "Text Categorization with Support Vector Machines: Learning with Many Relevant Features," *Proc. 10th European Conf. Machine Learning (ECML-98)*, Chemnitz, Germany, 1998.

[92] L. Bottou, C. Cortes, J.S. Denker, H. Drucker, I. Guyon, L.D. Jackel, Y. LeCun, U.A. Muller, E. Sackinger, P. Simard, and V. Vapnik, "Comparison of classifier methods: a case study in handwritten digit recognition," *Proc. 12th IAPR Int. Conf. Pattern Recognition, Conf. B: Computer Vision and Image Processing*, vol. 2, pp. 77–82, 1994.

[93] Z. Li, S. Tang, and H. Wang, "Pairwise coupling support vector machine and its application on handwritten digital recognition," *IEEE 2002 Int. Conf. Communications, Circuits and Systems and West Sino Expositions*, vol.2, pp. 1194–1198, 2002.

[94] E. Osuna, R. Freund, F. Girosit, "Training support vector machines: an application to face detection," *Proc. IEEE Conf. Computer Vision and Pattern Recognition* (*CVPR'97*), pp. 130–136, 1997.

[95] C. Papageorgiou, T. Poggio, "A pattern classification approach to dynamical object detection," *Proc. 7th IEEE Int. Conf. Computer Vision* (*ICCV*), vol. 2, pp. 1223–1228, 1999.

[96] M.P.S. Brown, W.N. Grundy, D. Lin, N. Cristianini, C.W. Sugnet, T.S. Furey, M. Ares Jr., and D. Haussler, "Knowledge-based analysis of microarray gene expression data by using support vector machines," *Proc. Natl. Acad. Sci. of the United States of America*, vol. 97(1), pp. 262–267, 2000.

[97] T. Jaakkola, M. Diekhans, D. Haussler, “A discriminative framework for detecting remote protein homologies, *J. Computational Biology*, vol. 7(1–2), pp. 95–114, 2000.

[98] O. Ivanciuc, "Applications of Support Vector Machines in Chemistry", *Reviews in Computational Chemistry*, vol. 23, pp. 291–400, 2007.

[99] L. Wang (Ed.), “Support Vector Machines: Theory and Applications (Studies in Fuzziness and Soft Computing),” Springer-Verlag, Berlin, Heidelberg, 2005.

[100] Chih-Chung Chang and Chih-Jen Lin, LIBSVM: a library for support vector machines, 2001. Software available at <http://www.csie.ntu.edu.tw/~cjlin/libsvm>. Last accessed on Oct 21 2007.

[101] Carl G. Looney, "A fuzzy classifier network with ellipsoidal Epanechnikov functions," Technical Report, Computer Science & Engineering Dept., University of Nevada, Reno, 2002.

[102] S.C. Lee and E.T. Lee, “Fuzzy Neural Networks,” In: [62], pp. 448–467.

[103] W. Siler, “Fuzzy Expert Systems and Fuzzy Reasoning,” John Wiley & Sons, Inc., Hoboken, NJ, USA, 2005.

[104] K. Fukunaga and P.M. Narendra, “A branch and bound algorithm for computing *k*-nearest neighbors,” *IEEE Transactions on Computers*, C 24, pp. 750-753, 1975.

[105] K. Fukunaga and R.D. Short, “Generalized clustering for problem localization,” *IEEE Transactions on Computers*, C 27, pp. 176-181, 1978.

[106] J.B. McQueen, "Some methods for classification and analysis of multivariate observations," *Proceedings of Fifth Berkeley Symposium on Mathematical Statistics and Probability*, pp. 281–297, 1967.

[107] J.M. Peña, J.A. Lozano, P. Larrañaga, "An empirical comparison of four initialization methods for the *K*-means algorithm," *Pattern Recognition Lett.* Vol. 20(10), pp. 1027–1040, 1999.

[108] C.G. Looney, "Interactive clustering and merging with a new fuzzy expected value," *Pattern Recognition Lett.* Vol. 35(11), pp. 2413–2426, 2002.

[109] W. Zhong, G. Altun, R. Harrison, P.C. Tai, and Y. Pan, "Improved *k*-means clustering algorithm for exploring local protein sequence motifs representing common structural property," *IEEE Trans. Nanobioscience*, vol. 4(3), pp. 255–226, 2005.

[110] J.C. Bezdek, "Fuzzy mathematics in pattern classification," *Ph.D. dissertation*, Cornell University, Ithaca, NY, 1973.

[111] J.C. Bezdek, R.J. Hathaway, M.J. Sabin, and W.T. Tucker, "Convergence theory for fuzzy *c*-means: counterexamples and repairs," *IEEE Trans. Systems, Man, and Cybernetics*, vol. 17(5), pp. 973–877, 1987.

[112] A. Rosenfeld, "Fuzzy digital topology," *Information and Control*, vol. 40(1), pp. 76–87, 1979.

[113] A. Rosenfeld, "The fuzzy geometry of image subsets," *Pattern Recognition Lett.*, vol. 2, pp. 311–317, 1991.

[114] J. K**.** Udupa and S. Samaraeskera, "Fuzzy connectedness and object definition: theory, algorithms and applications in image segmentation," Graphical Models Image Processing, vol. 58(3), pp 246–261, 1996.

[115] J. K. Udupa, L. Wei, S. Samarasekera, Y. Miki, M. A. van Buchem, and R. I. Grossman, "Multiple sclerosis lesion quantification using fuzzy connectedness principles," *IEEE Trans. Medical Imaging*, vol. 16, pp. 598–609, 1997.

[116] R. He and P. A. Narayana, "Automatic delineation of Gd enhancements on magnetic resonance images in multiple sclerosis," *Medical Physics*, vol. 29, pp. 1536–1546, 2002.

[117] G. Moonis, J. Liu, J. K. Udupa, and D. Hackney, "Estimation of tumor volume using fuzzy connectedness segmentation of MR images," *Amer. J. Neuroradiol.*, vol. 23, pp. 356–363, 2002.

[118] P. K. Saha, J. K. Udupa, E. F. Conant, D. P. Chakraborty, and D. Sullivan, "Breast tissue density quantification via digitized mammograms," *IEEE Trans. Medical Imaging*, vol. 20, pp. 792–803, 2001.

[119] J. K. Udupa, D. Odhner, and H. C. Eisenberg, "New automatic mode of visualizing the colon via CT," in *Proc. SPIE: Medical Imaging*, vol. 4319, San Diego, CA, pp. 237–243, 2001.

[120] J. Dehmeshki, H. Amin, W. Wong, M.E. Dehkordi, N. Kamangari, M. Roddie, J. Costelo, "Automatic polyp detection of colon using high resolution CT scans," *Proc. 3rd Int. Symposium on Image and Signal Processing and Analysis* (*ISPA*), vol. 1, pp. 577–581, 2003.

[121] F. Giorgini, A. Verrini, and S. Dellepiane, “A fuzzy approach to segment document images,” *Proc. Int. Conf. Image Analysis and Processing*, pp. 987–991, 1999.

[122] B. Prados-Suárez, D. Sánchez, and J. Chamorro-Martínez, “On Significant Crisp Representatives of Fuzzy Regions in Colour Images,” *IEEE Int. Fuzzy Systems Conf.* (*Fuzz-IEEE 2007*), pp. 1–6, 2007

[123] Y.-B. Lai, L.-S. Lan, M.-Y. Tsai, and C.-C. Chin, “On-line handwritten Chinese character recognition using a radical-based affine transformation,” *Int. Conf. Image Processing* (*ICIP’04*), vol. 5, pp. 2881–2884, 2004.

[124] Carl G. Looney, " Fuzzy Connectivity Clustering with Radial Basis Kernel Functions," *Pattern Recognition*, preprint, 2007.